NTNU – Trondheim
Norwegian University of
Science and Technology

Improved drilling process through the determination of hardness and lithology boundaries

Silje Marie Solberg

Earth Sciences and Petroleum Engineering
Submission date: May 2012
Supervisor: Pål Skalle, IPT

Norwegian University of Science and Technology
Department of Petroleum Engineering and Applied Geophysics

Abstract

The main objective of drilling a well is the potential economic profit. The total cost of a drilling operation result from a complex interplay of many factors (Graham and Muench, 1959). Work that can optimize some of these factors is desirable, and the need for information that can eliminate unfortunate incidents resulting in increased operational time and make the operation more efficient is constant.

Well cemented layers and the composition of the cemented materials are the main causes of hard stringers. Hard stringers may lead to severe downhole problems like washouts, severe local doglegs and keyseats. Such downhole problems are often related to the unexpected appearance of hard stringers and may cause the drill string to stick and result in lost time.
Hard and soft stringers may be detected through real-time drilling data. This is achieved by comparing different drilling parameters, like rotary speed (RPM), weight on bit (WOB) and block position (BPOS). A decrease in RPM followed by an increase in WOB indicates hard formations. However, manual analyses are time consuming and inefficient.

A modified and improved version of the hardness detection program previously developed by Solberg (2011) is presented in present thesis. The model is based on a simplified version of the rate of penetration (ROP) equation proposed by Bourgoyne and Young (1986). Drillability is the desirable result from the equation, as drillability is the inverse of hardness. Not all the functional relations that initially are part of the ROP equation have been assumed relevant for the detection of soft and hard stringers. Some of them alter only gradually, either with depth or as the drilling operation progresses, and do not affect the sudden change in drillability as the well is being drilled.

WOB, RPM and ROP (ΔBPOS/Δt) are drilling parameters chosen as relevant for present work. They are obtained through real-time drilling data and utilized in the calculations of drillability. Exponents related to the WOB and the RPM functions will frequently vary with the hardness in the formation. However, frequent manipulation of the exponents is difficult to achieve and only one soft and one hard formation exponent related to each exponent type have been applied.

The final result shows a plot of hardness variation with depth. The plot has been proved to correlate well with experienced hard stringers stated in the Final Well Report.

The program has been proved to be able to detect lithology transitions. The boundaries of particularly the Utsira Fm are evident on the hardness curve. The detection of Utsira Fm is enhanced by both gamma ray and sonic log from the same formation in wells nearby. Correlations between the two logs and hardness have been established. However, due to absence of sonic and gamma ray data from Well 0, the trustworthiness of the establishment is hard to evaluate.

Sammendrag

Drivkraften bak det å bore en brønn er den potensielle økonomiske profitten. Den totale kostnaden av en boreoperasjon avhenger av et komplekst samspill mellom flere ulike faktorer. Arbeid som kan optimalisere noen av disse faktorene eller kunnskap som kan hindre uheldige hendelser som fører til nedetid og kan gjøre boreoperasjonen mer effektiv er svært ettertraktet.

Harde formasjoner stammer i hovedsak fra godt sementerte lag. Mineralsammensetningen i bergarten er også av betydning. Harde formasjoner kan føre til alvorlige borehullsproblemer som utvasking, doglegs og keyseats. Slike borehullsproblemer oppstår ofte på grunn av uventede harde formasjoner og kan føre til at borestrengen setter seg fast eller resultere i nedetid.

Harde og myke formasjoner kan oppdages ved å bruke sanntids boredata som for eks. rotasjons hastighet (RPM), vekt på biten (WOB) og blokkposisjonen (BPOS) og studere sammenhengen mellom dem. Minkning i RPM sammen med økning i WOB indikerer harde formasjoner. Imidlertid er slike manuelle analyser tidkrevende og lite effektive.

En modifisert og forbedret versjon av deteksjonsprogrammet tidligere utviklet av Solberg (2011) er presentert i denne masteroppgaven. Modellen baserer seg på en forenklet versjon av penetrasjonshastighetslikningen (ROP likningen) lagt fram av Bourgoyne og Young (1986). Borbarhet er det ønskelige resultatet fra likningen siden hardhet er den inverse av borbarhet. Ikke alle subfunskjonene som er med i den opprinnelige ROP likningen har blitt ansett relevante for påvisning av harde og myke formasjoner. Noen av dem endrer seg kun gradvis, enten med dyp eller som boreprosessen forløper, og påvirker ikke den brå endringen i hardhet.

RPM, WOB og ROP(ΔBPOS/Δt) er boreparametre valgt relevante for denne masteroppgaven. Disse parametrene oppnås gjennom sanntidsdata og er brukt i beregningen av borbarhet. Eksponenter relatert til WOB og RPM funksjonene vil variere med hardheten i formasjonene, men slike endringer av eksponenter er vanskelig å oppnå. Kun en myke og en hard formasjonseksponent relatert til hver eksponenttype har blitt brukt.

Det endelige resultatet viser et plot av hardhetsendring med dyp. Det har blitt påvist at plottet stemmer overens med harde formasjoner erfart under boreoperasjonen og notert i Final Well Report.

Programmet har vist seg å kunne påvise litologioverganger. Formasjonsgrensene av spesielt Utsira Fm er tydelig vist på hardhetskruven. Påvisningen av Utsira Fm er forsterket ved å se på gammastråle- og sonicloggene i samme formasjon fra brønner i området rundt. Sammenheng mellom hardhet og de to loggene har blitt stadfestet, men grunnet ingen tilgang til sonic- og gammastråleloggen i vår brønn er det vanskelig å evaluere hvor sikker denne sammenhengen er.

Acknowledgement

This report is a master thesis in Drilling Technology at the University of Science and Technology (NTNU) the spring 2012. The report has been written by Silje Marie Solberg who is a 5th year student at the Department of Petroleum Engineering and Applied Geophysics with specialization within drilling. Associate Professor Pål Skalle has been the supervisor for present master thesis.

I am sincerely and heartily grateful to my supervisor, Pål Skalle, for the feedback and guidance he showed me throughout my master thesis. Besides I would like to thank Sverre Ola Johnsen and Eirik Graue for providing me great information resources. I am also truly indebted and thankfulI to other professors at NTNU and especially fellow students who have been most helpful and supporting during my writing of this thesis.

Trondheim, 2012

Silje Marie Solberg

Table of Content

1 Introduction

Knowledge that optimizes the drilling process is important when drilling a well. The enterprising factor in the petroleum industry is the potential economic profit. A well that produce an acceptable amount of oil or/and gas that gives an income that exceeds the expenses of drilling a well is recognized as a successful well. Lost time increases the expenses of drilling a well drastically due to that a drilling operation in the North Sea costs approximately 2 MNOK per day. Information that may prevent severe destructive incidents and minimizes the operational time is therefore extremely desirable.

Sediments which are well cemented and consolidated are referred to as a hard rock. Most sedimentary rocks appear as thin layers or stringers due to the sedimentation process. Sudden change in hardness when drilling a well may cause severe problems during the drilling process and in worst case lead to an unwanted stop in the drilling operation. When drilling into a harder formation, the rate of penetration tends to decrease. The driller will then normally increase the weight on bit to access the harder formation. Too much weight on bit may buckle the drill string and eventually lead to too large side forces and washouts. Unwanted doglegs may also appear when drilling into harder formations. Severe doglegs may cause damage to the equipment and lead to operational failure. At worst case the planned total depth is not reached.

Present master thesis will look at hard and soft stringers` effect on the drilling process and predict hard and soft formations from real-time drilling data. A program will be proposed to make the prediction based on real-time drilling data where weight on bit, rotary speed and rate of penetration are relevant data applied. Present work will also compare the predicted hardness with the lithology observed in the formation to see if any correlation can be established. The gamma ray and the sonic log will also be studied to see if there can be established evidently correlation between gamma ray and hardness and/or sonic log and hardness. A literary study will also be done to achieve a better understanding of the mentioned topics.

The main objective of present thesis is to enable elimination of the above mentioned downhole problems in the future. A short term and more realistic goal is to be able to predict hard and soft stringers to avoid unexpected and unwanted incidents during drilling.

2   Relevant Published Knowledge

Detection of hard and soft stringers is complex and difficult to achieve. As drillability is an indicator of hardness it is vital to gain great knowledge about drillability to obtain the most accurate result. To understand the reason for present work it is also essential to be aware of the severe damage hard and soft stringers may cause.

2.1   Geological causes of hard and soft formations

The geological causes of soft and hard formations are mainly due to the degree of cementing. Well cemented quartz sandstones are harder than looser cemented sandstones. Rocks consisting of calcite or other carbonates are soft. The mineral composition also affects the hardness of the rock. Clean quartz sandstones are harder than arkosic (sandstones with feldspar) and greywacke (sandstones containing a lot of clay). However, the most important cause of hard and soft formations is most likely due to the degree of cementing and the cemented material (Personal comments; Johnsen, 2011).

2.2   Negative effects of soft and hard stringers on the drilling operation

This sub chapter is an extended version of the project by Solberg (2011).

Drilling hard and very hard, usually abrasive, formations result in the most difficult problems in the drilling industry despite the developments and improvements of drilling tools, equipments, machines and techniques. Hard formations leading to reduction in penetration rate and bit footage attained result in more frequent round trips which are a significant expensive factor when considering drilling costs (Saif, 1982).

Lack of knowledge of the change in hardness in the formation may cause several problems during a drilling operation. These unfortunate incidents may occur at three different places in the well, either on the borehole wall, down in the hole or it could lead to wear of the equipment and eventually equipment failure.

2.2.1   Equipment failure

Drill string failure: When the rock`s resistance to penetration increases, the driller tends to put on more weight on the bit. Enlarged weight on the bit may lead to too high torque. Wrong torque may wear the drill string and result in a hole in the string (Personal comments: Skalle, 2011). According to Head (1951), hard formations are most effectively drilled using rotational speeds of 40 to 100 revolutions per minute. Due to physical limitations imposed by the

drilling equipment, the speed cannot be increased in these formations. It could lead to premature failure of the drill pipe (Head, 1951).

Low ROP: Too little knowledge about the formation being drilled may lead to the wrong choice of bit. Incorrect bit type causes low ROP and eventually equipment failure.

2.2.2 Downhole problems

Washouts: Washout is an enlarged region of the wellbore (Schlumberger[1], 2011). When too much weight is put on the bit to enter a harder formation, the pipe will tend to buckle. When a soft formation is situated above a hard stringer the buckled pipe may erode into the side of the borehole wall in the softer formation. This results in a magnified region of the wellbore when the pipe is being rotated. See Figure 2-1.
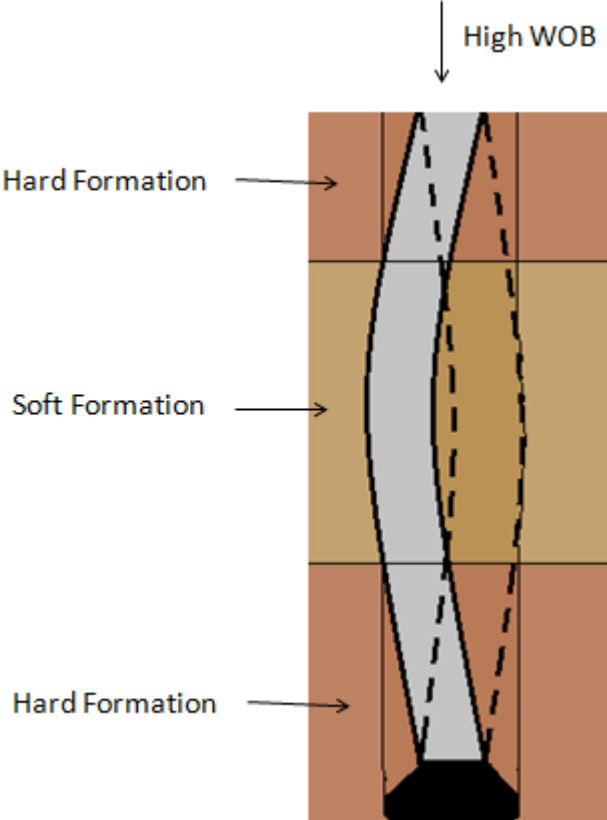

Figure 2-1 Washout due to a buckled drill string caused by too much weight on bit.

Washouts may cause the pipe to stick at the ledges and the shoulders of the borehole wall when pulling out or tripping in.

Dogleg: A dogleg may be created intentionally by steerable tools and directional drillers. However, when drilling from soft to harder formations an unwanted dogleg may appear. Such

local dogleg is referred to as a section of hole that changes direction faster than anticipated or desired (Schlumberger[2], 2011).

Doglegs are associated with several problems. The wellbore will not be located at the planned path if an unwanted dogleg occurs. This may lead to that the planned casing string no longer fits the wellbore. The casing may also wear quicker due to contact forces between the drill string and the inner diameter of the casing appearing due to doglegs. A relatively stiff bore hole assembly (BHA) may not fit through the dogleg section drilled with a limber BHA. Unwanted doglegs increase the possibility of the drill string being stuck and there will be a greater overall friction to the string. In worst case, the planned total depth is not reached (Schlumberger[2], 2011).

High local doglegs provide stresses into the drilling system that can rapidly accelerate fatigue of the BHA components and connections. Such doglegs may appear when entering or exiting a calcite interval. The bit can be forced aside to create severe local doglegs. Figure 2-2 illustrates high local dogleg (HLD). While drilling the Troll field, several catastrophic downhole BHA failures, like cracked component and mud intrusion events, turned out to be results of high local doglegs. However, there were also similar incidents with no indications of a local dogleg in the vertical plane (Hood, Hovden and Heisig et al., 2003).
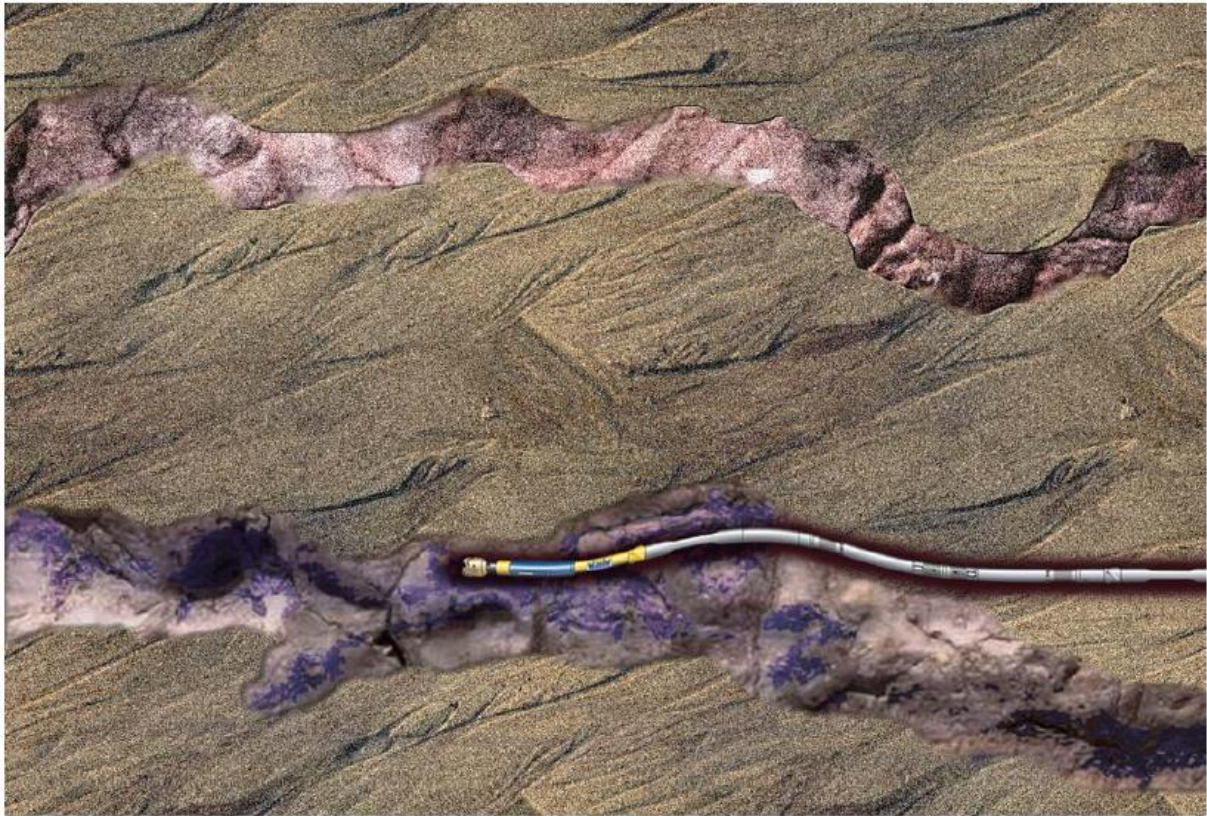
Figure 2-2 Artistic illustration of HLD developed at the surface of a calcite cemented stringer (Hood, Hovden and Heisig et al., 2003)

Keyseat: Doglegs may also result in keyseating. Keyseats appear when the drill string causes repeated abrasion at a particular location of the dogleg. It may also occur when a hard formation ledge is left between two softer formations that enlarge with time. Dogleg and keyseats are illustrated in Figure 2-3.
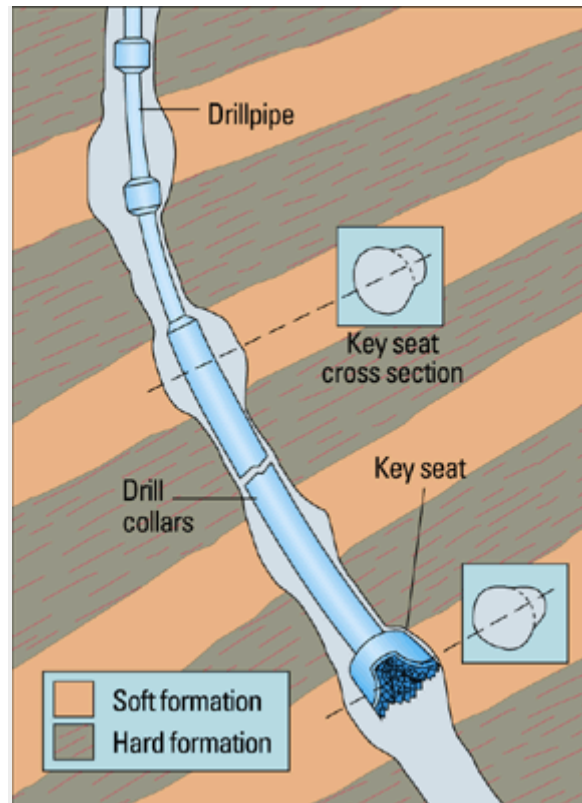
Figure 2-3 Doglegs may result in keyseats in soft formations (Schlumberger[3], 2011)

Keyseating may lead to the BHA being stuck when trying to pull it through the section. Also other larger diameter drilling tools may get stuck in the keyseat when they are being pulled out. Such tools are tool joints, drill collars, stabilizers etc (Schlumberger[3], 2011).

2.3 Negative effects from shale on drilling operation

Sloughing and swelling of shale are the two major problems encountered when drilling a well. Shales make up 75% of the drilled formations and is the cause of 90% of the wellbore instability problems . Some shale sections contain hydratable clays, which continually absorb water and swell and slough into the hole. These formations, known as heaving shales, may result in high cost of drilling the hole and also cause other hole problems like pipe sticking, excessive solid build up in the mud and hole bridging. Sometimes it could also lead to abandoning the well due to the difficulty of reaching the planned total depth (Talabani, Chukwu and Hatzignatiou, 1993).

2.4 Drillability

Rock drillability defined by Somerton, Esfandiari and Singhal (1969), is the volume of rock drilled per unit of energy input. Overton (1973) defined drillability as the rate at which a given rock may be penetrated. As the first bit came to the world, people started investigating

the bit performance focusing on the interaction between bit and rock. This investigation is still ongoing and the complete understanding of rock-bit interaction still has a long way to go (Wu, Hareland, and Rashidi et al., 2010). Drillability is an indicator of drilling complexity, drilling performance and cost according to Albertin, Petmecky and Jay (2003). Several different methods have been applied through the history of drilling to determine drillability or express drillability in terms of other drilling parameters. A short summary of some studies on drillability are further described in this chapter.

Drillability indicates whether the penetration is easy or hard. Therefore will an accurate prediction of the drillability give a good picture of the hardness in the drilled formation,

$$Hardness = \frac{1}{Drillability}$$
(2-1)

However, Head (1951) conducted limited tests to determine any relations between drillability and hardness in the formation and concluded that no such relationship could be established based on the results. Head (1951) made a classification of geological formations based only on the relative efficiency at which these formations could be drilled. He proved the classification to be consistent with actual field drilling practices. The drillability seemed to be more related to the manner which the hard crystals are bound together than to the hardness (Head, 1951).

Drillability cannot be measured by logging tools, but is an estimation based on other drilling parameters according to Cheniany, Khoshrou and Shahriar et al. (2010). These drilling parameters are divided into two categories, controllable and uncontrollable parameters. Bit type and bit diameter, rotational speed, thrust, blow frequency and flushing are parameters controlled by the driller while rock properties and geological conditions are uncontrollable parameters. Head (1951) stated that the geological formation encountered while drilling a well is the only factor that is truly uncontrollable. Sticky and sandy shale, gravel, salt, plastic clay, hard and soft sand, sandstone, limestone, dolomite and granite are common formations drilled. Each formation has characteristics which affect its resistance to penetration.

Somerton (1959) investigated the controlling rates of bit penetration under laboratory conditions and the effects of rock strength and bit wear on drilling rates. He also analyzed the cuttings to determine the character of breakage and comparing with other producing rock

breakage methods. Somerton studied some variables controlling bit penetration rates conveniently by dimensional grouping. The equation consisted of rate of penetration (R), bit diameter (D), rotary speed (N), effective weight on bit (F), rock strength parameter (S) and a constant (C) and an exponent (a) to be determined experimentally.

$$R = C\ D\ N\ (\frac{F}{D^2\ S})^a \qquad\qquad (2\text{-}2)$$

The rock strength is the only variable difficult to evaluate (Somerton, 1959). Rock strength was by Spaar, Ledgerwood and Christensen et al. (1995) found to correlate well with the overall measures of bit effectiveness. Formation strength correlates to formation drillability, which is best determined from unconfined compressive strength and the angle of internal friction (Spaar, Ledgerwood and Christensen et al., 1995).

Gstalder and Raynal (1966) stated that drillability of rocks cannot be defined in an absolute manner by one single quantity or a single test. Gstalder and Raynal (1966) considered simple tests, like modified Schreiner tests, performed on rocks to give a measure of rock drillability. Test results showed that hardness can be used as a measure of breaking strength. There were proved useful relationship between hardness and other physical quantities such as sonic velocity. It may be possible to deduce rock drillability from sonic log data provided that a mineralogical factor is taken into account (Gstalder and Raynal, 1966).

After analyzing different formulas for drillability, Markman (1971) found that they either take account for only a limited number of influencing factors or they are not applicable to rotary borehole drilling conditions. Dvornikov (1964) constructed graphs and attempted to derive formulas that to a degree expressed the drilling process. He based his work on experimental data from Soviet and foreign investigators. In 1971 it had so far been impossible to derive one single formula that related all the quantities influencing the drilling operation. However, functions which took account for the most important factors in the drilling and cutting processes and were accurate enough for engineering calculations had been made (Markman, 1971).

Overton (1973) proposed a dimensionally derived rock drillability equation. To make a generalized drillability equation that is portable, it was necessary to make an analysis of the interaction of the rotating bit, the circulation system and rock properties. Many equations are in use in rotary drilling. Dimensional analysis can simplify the situation of numerous

equations to formulate a generalized equation for all rock bits. The equation requires the determination of ten measurable variables, two coefficients that depend upon rotary bit and mud practice and two parameters that depend upon the composition of the rock. Some measurable variables are rotary speed, weight on bit, hole diameter, drilling depth, differential pressure and tooth height. The parameters that cannot be obtained through measuring or calculations must be determined by experiment in either lab or the field (Overton, 1973).

Hongjin stated in 1986 that all research efforts on drillability made up until that year was based on assumptions of a homogeneous formation inferred from representative rock samples. The exact opposite is normally the case. The formations drilled are mainly heterogeneous. Hongjin (1986) introduced a statistical approach for studying the drillability that comes from experimental observation of a large number of samples. The approach gives a quantitative correlation of different parameters and can treat the formations studied as heterogeneous formations. Hongjin (1986) also proposed an empirical equation of drillability made statistically varying with depth. It generalizes the sample population taken from the formation and represents the characteristic of individual heterogeneous formations. The drillability can then be calculated mathematically and effortlessly and gives a more accurate result than a rough estimate (Hongjin, 1986).

Albertin, Petmecky and Jay et al. (2003) derived the drillability index from visualization of large 3D seismic data volumes. The drillability emphasizes difficult drilling areas in particular, which often are de-emphasized in pressure data alone.

Prasad (2009) presented a model where drillability was described in terms of eight simple physical, mechanical and micro-structural properties. The relevant rock properties were density, porosity, compressional and shear wave velocities (sonic), unconfined compressive strength, Mohr friction angle, mineralogy and grain sizes. These properties were possible to achieve either from the log data or from the core testing in a commercial laboratory. The rock properties were compiled and normalized to range from 1 to 8 where 1 represented very soft rock and 8 represented very hard rock. The plot, called a "spider plot", characterizes drillability (Prasad, 2009).

Mathematical equations have been proposed by several to calculate the drillability in the formation. Many of these use the rate of penetration to make an accurate prediction. Due to the great coherence between drillability and rate of penetration it is necessary to look at the

change in rate of penetration to be able to detect hard and soft formations (Wu, Hareland, and Rashidi, 2010).

2.5 Mathematical Models of Rate of Penetration to compute hardness

There is proved great coherence between rate of penetration and drillability. Drillability and penetration rate can be defined in the same terms where drillability indicates wether the penetration is easy or hard, while penetration rate designate whether the penetration is fast or slow.

The factors controlling ROP are numerous and rely on many other factors. Some of these factors are not complimentary, but complex and nonlinear, meaning that an increase in one may lead to a decrease in another. An increase in weight on bit may increase ROP for some time, but may cause the bit to wear and dull faster. This tends to reduce ROP in the long run, and making it hard to optimize the drilling operation. ROP is difficult to predict and is typically obtained real-time (Alum and Egbon, 2011). Previous work done on modeling ROP usually focus on the mechanical parameters (weight on bit, rotary speed, bit type, bit dull, drillability). The hydraulic parameters are paid less attention (annular velocity, bit hydraulics, differential pressure, bottom hole cleaning, solid percentage in the mud, mud type and properties). However, it was proved by Alum and Egbon (2011) that especially drilling fluid properties affect the ROP considerably.

Prediction of penetration rate has always been one of the most essential issues among drilling engineers. The prediction makes it possible to achieve the minimum cost per foot by selecting the optimum drilling parameters (Bahari and Baradaran, 2007). Many different methods exist for optimizing drilling parameters and operations. Drill-off tests, previous experience, monitoring, analyzing parameters, engineering judgment and modeling are some of these processes. However, such methods require great resources (rig time, skilled engineering time etc.) and the result may only be relevant to optimize that specific situation (Koederitz and Johnson, 2011).

Drilling simulation software is one way of improving drilling operation by predicting and comparing different drilling scenarios which helps optimizing the drilling process. An inseparable part of the drilling simulation software is to model the rate of penetration. Improvements in the prediction of penetration rate are therefore valuable for the drilling industry (Wu, Hareland and Rashidi, 2010).

Several mathematical models that attempt to combine the earlier mentioned drilling parameters have been projected. Such models are used to apply formal optimization methods to choose the correct weight on bit and rotary speed to obtain minimum cost per foot.

Two of these models are further described of which one of them have been applied in present master thesis.

2.5.1   Normalized Rate of Penetration

Normalized rate of penetration (NROP) is a normalization of the effect different drilling parameters have on rate of penetration described by a drilling equation. The result is a plot of penetration rate that is not affected by weight on bit, rotary speed or hydraulics which can be important in control or directional drilling. The NROP plot shows what the drilling rate should be if the other parameters are held constant and by that more accurately identifies the formation characteristics. NROP makes it easier to identify lithology changes and pressure transition zones. Correct use of NROP reduces drilling expenses due to less number of logging trips, minimized trouble time through detection of pressure transition zones and encouraged near balanced drilling to achieve faster penetration rate. The normalized rate of penetration is expressed as follows;

$$NROP = ROP \; x \; \frac{(W_n - M)}{(W_o - M)} \; x \; \left(\frac{N_n}{N_o}\right)^r \; x \; \frac{(Pb_n \; x \; Q_n)}{(Pb_o \; x \; Q_o)} \qquad (2\text{-}3)$$

ROP – observed rate of penetration

Wn – normal bit weight

Wo – observed bit weight

M – Formation threshold weight

Nn – normal rotary speed

No – observed rotary speed

r – Rotary exponent

Pbn – normal bit pressure drop

Pbo – observed pressure drop

Qn – normal circulation rate

Qo - observed circulation rate

The NROP plot is very effective for lithology prediction based on the drillability of the formations. The plot should show significantly slower drilling rate in sand-shales than in sand

zones at the same depth. A sudden change in penetration rate suggests sandy formations when drilling the base formation. The NROP plot is an excellent lithology correction tool in sand-shale sequences, even when actual penetration rate plots fail to identify zones (Provost, 1987).

2.5.2   Rate of Penetration model by Bourgoyne and Young

Bourgoyne and Young proposed perhaps the most complete mathematical drilling model for rolling cutter bits (Bourgoyne, Millhelm and Chenevert et al., 1986). It has been proved later that the same model can be applied for bits operating in the industry today (Personal comments: Skalle, 2012).

The change in rate of penetration has by Bourgoyne and Young been expressed as a function of eight different drilling parameters expressed as follows,

$$R = (f_1)(f_2)(f_3)\dots(f_8) \tag{2-4}$$

where the eight functional relations define formation drillability, decrease in penetration rate with depth, increase in penetration due to under-compaction and change in penetration due to mud weight, weight on bit, rotary speed, tooth wear and jet impact force. Drillability was presented in chapter 2.3. Some other factors mentioned above are further described below.

Two of the influencing factors model the effect of compaction on the penetration rate. One of them accounts for the rock strength increase due to compaction with depth. Naturally, deep rocks will be more compacted than the above layers and therefore harder to drill than similar shallower formations. Drillability of a sample of deep and compacted rock will generally increase when the sample is brought to the surface compared to its original location (Garnier and Van Ingen, 1958).The second compaction factor models the effect of under-compaction experienced in abnormally pressured formations. Normally in a compacted sequence, the rock grains are in contact with each other and the weight of the overlying sediments is supported by the rock matrix. Sediments get normally compacted when the rate of burial is slow, the rocks have adequate permeability to allow fluids to migrate and the system allows the migrating fluids to escape. Under-compaction happens when the mentioned conditions are not met. Quick burial together with low permeability of claystones and shales result in that the water within the sediments is unable to escape fast enough to obtain normal compaction. The overlying rocks will therefore be supported by both the rock matrix and the interstitial fluids which result in an over pressured formation. Deeper burial results in higher formation

pressures if the fluids cannot escape. All subsequent overlying sediments will be supported by the interstitial fluids while the matrix stress remains constant (Pore pressure, 2012).

Both weight on bit and rotary speed have great impact on the penetration rate. Numerous of authors have studied their influence, both in the field and in the laboratory. No significant ROP is possible unless threshold bit weight is applied. The penetration rate increases as the bit weight increases and/or the rotary speed increases if all other parameters are held constant. The great impact these two parameters have on rate of penetration is also concluded by other scientists. To determine the relation between rotary speed and rate of penetration, Bielstein and Cannon (1950) made an analysis on limited tests that had been run on two-element jet rock bits in the Taylor shale. The analysis reveals that the drilling rate increases as the rotary speed is increased and changes at the rate of approximately 1:2. The relationship established by these analyses may be limited to high drillability formations. Bielstein and Cannon (1950) also conducted controlled tests on various bit designs in soft and medium hard formations to determine the relation between bit weight and rate of penetration. The tests were conducted in the same formations as for the rotary speed tests. Analysis of the data shows that the drilling rate is directly proportional to the weight on bit when using the two-element jet rock bits, although some variation from the direct proportionality exists. Limited tests indicate that the rate of penetration increases as the weight on bit is increased and changes at the rate of 1:4 when using two-element conventional rock bits in medium-hard formations. Bielstein and Cannon (1950) concluded that rate of penetration is a function of both rotary speed and weight on bit. The relationship of bit weight to drilling rate varies with the formation hardness.

It is assumed that the effects of the different drilling variables are all independent of one another. These functional relations (f_1, f_2, etc.,) are usually based on trends observed either in the laboratory or in the field (Bourgoyne, Millhelm and Chenevert et al., 1986).

The drilling parameters or coefficients represented in the model of Bourgoyne and Young are all dependent to the ground formation types and can be verified by previous drilling experiences in the field. The modeling of drilling behavior in a specific formation is accomplished by selecting the constants a_2 through a_8 which all are related respectively to each function mentioned above (Bourgoyne and Young, 1974). The constants can be determined from knowledge of the type of lithology to be encountered. Frequent change in lithology with depth makes it difficult to evaluate the correct value of the exponent in each

formation type. The process of how to determine these constants has great impact on the accuracy of the model. Bourgoyne and Young suggested multiple regression analysis of detailed drilling data taken over short depth intervals. The accuracy of the calculation can be improved if the constants, a_2-a_8, are obtained through a multiple regression analysis of field data previously obtained in the area (Bourgoyne and Young , 1973). However, this method is limited to the number of data points (Bahari, Bahari and Moharrami, 2008). Bahari and Baradaran (2007) applied non-linear least square data fitting with trust-region method to this problem. This method diminishes the amount of square errors function and is one of the optimization algorithms.

2.6 Sonic Log as an indicator of lithology

According to Aron, Chang and Codazzi et al. (1997) the new sonic-while-drilling tool can obtain real-time formation slownesses over a wide measurement range. Real-time sonic logs allow for real-time decision-making and provide valuable data for the drilling operation. Such measurement has earlier only been achievable in hard rock due to that it is more challenging to measure compressional slowness in a slow formation due to later formation arrival in time and often lower amplitude. Measuring compressional and shear slownesses in hard rock can be used to identify lithology in the formation. In general, logging-while-drilling and wireline logs agree with real-time sonic log. However, experience made by Aron, Chang and Codazzi et al. (1997) shows that some depth intervals, especially in shale, have different measurements.

Since the beginning of 1960's, compressive strength has been successfully related to drillability. Gstalder and Raynal (1966) studied the relation between hardness and compressional velocities and concluded that the rock hardness increases as the compressional velocities was increased. Somerton, Esfandiari and Simghal (1969) made the same conclusion when he looked at the relation between drilling strength and compressional velocity. The drilling strength increased with an increase in compressional velocity. Spaar, Ledgerwood and Christensen et al. (1995) stated existence of clear correlation between rock hardness and compressional waves. As travel times become faster, the rocks got harder. However, the velocities of compressional waves are indeed sensitive to the fluid in the formations. This can especially be problematic if the formation fluid is gas due to that the gas greatly reduces compressional wave velocity. A hard formation containing gas would then appear to be weak. Shear waves on the other hand do not get affected by formation fluids. Correlation between

formation strength and shear wave velocities represents a great improvement over compressional wave techniques (Spaar, Ledgerwood and Christensen et al., 1995).

The relations between elastic moduli and sonic velocity are well known. Evidence indicates the function of sonic velocity could be introduced into rock drilling equations to account for rock strength term (Somerton, Esfandiari and Simghal., 1969).

Elkington et al. studied the relationship between diametrical point load tests performed on different rocks and log properties. They concluded that of all the logs they had analyzed, the neutron, gamma ray and sonic log had the greatest rock strength prediction potential (Onyia 1988). Onyia (1988) discussed the relationship between rock drilling strength and some wireline log properties. The models developed and described by Onyia (1988) showed good correlation between sonic travel times and rock strength.

Andrews, Nygaard and Engler et al. (2007) developed a correlation between drillability and sonic logs for different lithology types using data from 10 wells in North America. The gamma ray log was employed in conjunction with drilling data in the calculation of drillability. The drillability from penetration rate models was back calculated from bit design, field wear, meter by meter operating parameters, formation types and pore pressure. The drillability was then compared with the sonic logs for different lithologies defined by the gamma ray log. It was proved that different formation types showed clearly diverse correlations for the normalized correlations between drillability and sonic logs. More than 100 000 data points were statistically analyzed and used in the evaluation. The predicted apparent rock strength from sonic log was proved to correlate well with the estimated apparent rock strength when using a reference well that closely matches the characteristics of the planned well. The predicted apparent rock strength from sonic logs was not affected by problems encountered while drilling. The equation developed by Andrews, Nygaard and Engler et al. produced similar results to Onyia`s correlation which confirms that these correlations can be used in wider geographically areas (Andrews, Nygaard and Engler et al., 2007).

2.7 Gamma Ray as an indicator of rock lithology

The gamma probe (sonde) measures the natural radioactive radiation from the formation. Lots of clay minerals are radioactive while quartz sandstones and carbonates are not. The gamma log is widely used as a clay indicator (Langeland, 1992).

Almost all rocks contain some radioactive elements. Potassium (K^{40}), thorium and uranium cause almost all radioactivities in the earth. Quartz sandstones and carbonated contain often very little radioactivity while dolomites may contain some radioactive minerals. Mica and feldspar contain huge amounts of potassium. These mineral groups turn into clay minerals through aging/maturing. Even though not all clay minerals are radioactive initially, adsorption of ions of radioactive minerals may make them contribute to make the clay/shale radioactive (Langeland, 1992).

The gamma-log may contribute to determine the lithology in the formation in addition to looking at other factors like cuttings and already known geology. The log is utilized to separate between radioactive and not radioactive zones which often indicate fissility and clean zones (Langeland, 1992).

Natural gamma-ray borehole logging is an acknowledged technique for determining uranium deposits and obtaining lithographic data. Spectral gamma-ray borehole logging is a refinement of the technique and categorizes gamma-rays based on their energies. The energies are results of potassium (K), uranium (U) and thorium (T) in the formation. Spectral gamma-ray logging allows the source of gamma-rays to be identified based on the type of energy the radioactive element provides. Each radioactive element emits gamma-rays with distinct, characteristic energies (Young, 1980).

Gamma ray log readings were used as a simple approach for shallow wells in Alberta, Canada in 2009 to determine the lithology in the area. It was proved to be in generally good agreement with shale and sand lithology content. It was seen that the gamma ray method matched for shale and sand sequences and mixtures. However, gamma ray alone, could not recognize formations of limestone and dolomite (Rashidi, Hareland and Shirkavand, 2009).

3 On-line model of hardness

Both physical and mathematical models can be used for detection of hardness. In both cases, several drilling parameters have to be taken into consideration to make the most accurate prediction. The accuracy of the prediction increases with the amount of drilling parameters considered.

3.1 Physical understanding

By analyzing the curves of different drilling parameters in the same real-time drilling data window, hard and soft formations may be indicated. Especially the coherence between WOB and BPOS is of significance. Correlation between the reduction of the block position speed and the increase in weight on bit and vice versa is seen in Figure 3-1, where both soft and hard formations are recognized.
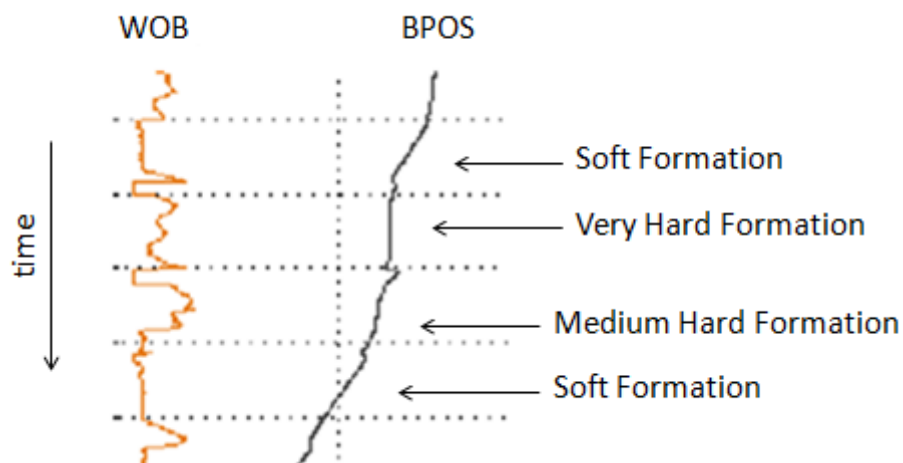

Figure 3-1 WOB and BPOS are plotted vs. time. A reduction in block position speed together with an increase in weight on bit indicates hard formations (Solberg, 2011).

Hard formations are indicated by increase in weight on bit when the speed of the block is decreased. However, the purpose of present work is to attain prediction of a formation without analyzing it in advance. This may be achieved by using mathematical models (Solberg, 2011).

3.2 Mathematical model

The Bourgoyne and Young`s model presented in chapter 2.5.2 has been applied and analyzed in present master thesis due to relevant data available through real-time drilling data.

3.2.1 Relevant functional relations

Equation 2-4 from chapter 2.5.2 has been applied in the calculations of drillability. Equation 2-1has been used to compute hardness from drillability.

However, not all parameters affecting rate of penetration (equation 2-4), and therefore drillability, are of interest in present work. All parameters modifying the drillability only gradually are considered constant and therefore neglected.

In addition to drillability, changes in penetration rate due to depth compaction, weight on bit and rotary speed are the functional relations selected relevant in equation 2-4.

Formation drillability;

$$f_1 = K \qquad (3\text{-}1)$$

K - Drillability

- Depth compaction factor;

$$f_2 = e^{2.303\, a_2\, (10000 - D)} \qquad (3\text{-}2)$$

D - Vertical depth [ft]
a2 - Depth correction exponent

The number 2.303 may be ignored due to that the exact values of drillability is of no interest.

- Weight on bit factor;

$$f_5 = \left[\frac{\left(\frac{W}{d_b}\right) - \left(\frac{W}{d_b}\right)_t}{4 - \left(\frac{W}{d_b}\right)_t} \right]^{a_5} = [W]^{a_5} \qquad (3\text{-}3)$$

W - Weight on bit [1000 lbf]
d_b - Bit diameter [in]
$(W/d_b)_t$ - Threshold bit weight per inch of bit diameter at which the bit begins to drill, 1000 lbf/in
a5 - Weight on bit exponent

The threshold bit weight is often small, especially in soft formations, and is assumed to be neglected. The value 4 in the denominator is a conversion constant and may also be ignored. The calculations are done in intervals using the same bit size. Since the exact value of drillability is of no interest, the bit diameter may also be neglected.

- Rotary speed factor;

$$f_6 = \left(\frac{N}{60}\right)^{a_6} = [N]^{a6} \tag{3-4}$$

N - Rotary speed [rpm]
a6 - Rotary speed exponent

The value 60 in the denominator is a conversion factor and has been neglected.

After the neglecting and the assumptions being made, the equation of rate of penetration is reduced to;

$$\mathrm{ROP} = (f_1)(f_2)(f_5)(f_6) = (K)\mathrm{x}\,(W)^{a_5}\mathrm{x}\,(N)^{a_6}x\,(e^{a_2(10000-D)}) \tag{3-5}$$

ROP, WOB and N are known from real-time drilling data. Drillability can be expressed in terms of equation 3-6 when rearranging the rate of penetration equation;

$$\mathrm{K} = \frac{ROP}{(W)^{a_5}x\,(N\,)^{a_6}x\,(e^{a_2(10000-D)})} \tag{3-6}$$

3.2.2 Determining relevant exponents

In practice, it is prudent to select the best average values of the constants a_2 through a_8 for the formation types being drilled (Bourgoyne, Millhelm and Chenevert et al. 1986).

If all the other functional relations are neglected except f_2, equation 2-4 can be rewritten into equation 3-7.

$$ROP = f_2 \tag{3-7}$$

A_2 can be found through linear regression by plotting vertical depth versus the natural logarithm of ROP. Combining equation 3-6 and 3-7 and applying the natural logarithm on both sides results in equation 3-8.

$$\ln(\mathrm{ROP}) = \ln(\mathrm{ROP}_0) + (2.303\,a_2\,1000 - 2.303\,a_2\,D)\ln(e)$$

$$= [\ln(\mathrm{ROP}_0) + 2.303\,a_2\,1000] - 2.303\,a_2\,D \tag{3-8}$$

A trend line may be established to obtain the exponent, a_2, which best fit the curve. The trend line may be expressed as a linear equation,

$$C = B + Ax \tag{3-9}$$

Comparing equation 3-8 and 3-9, it can be recognized that,

$$B = \ln(ROP_0) + 2.303\,a_2\,1000 \tag{3-10}$$

and

$$A = -2.303 \, a_2 \tag{3-11}$$

Figure 3-2 shows the vertical depth plotted versus the natural logarithm of ROP in the 24" bit section.
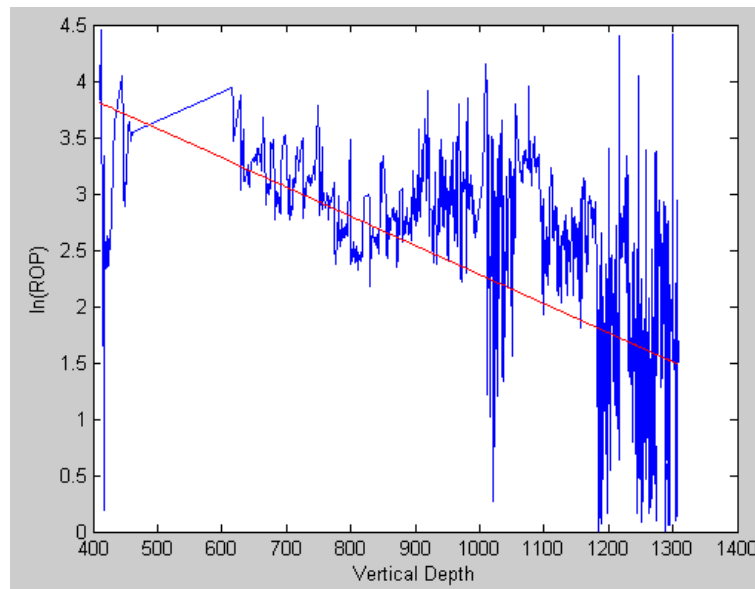

Figure 3-2 Well 0. 24" bit section. Vertical depth is plotted versus the natural logarithm of ROP. The red line illustrates the trend line characteristic for this plot.

The red line represents the linear regression line of the plot and is referred to as the trend line. The line has a slope equal to A and intersects the y-axis (x=0) at ln(ROP) equal to B.

A = - 0.0026 in the 24" bit section. A_2 is found to be equal to 1.129 x 10^{-3} by using equation 3-11.

The data are recorded from the 17 ½" section in Figure 3-3.
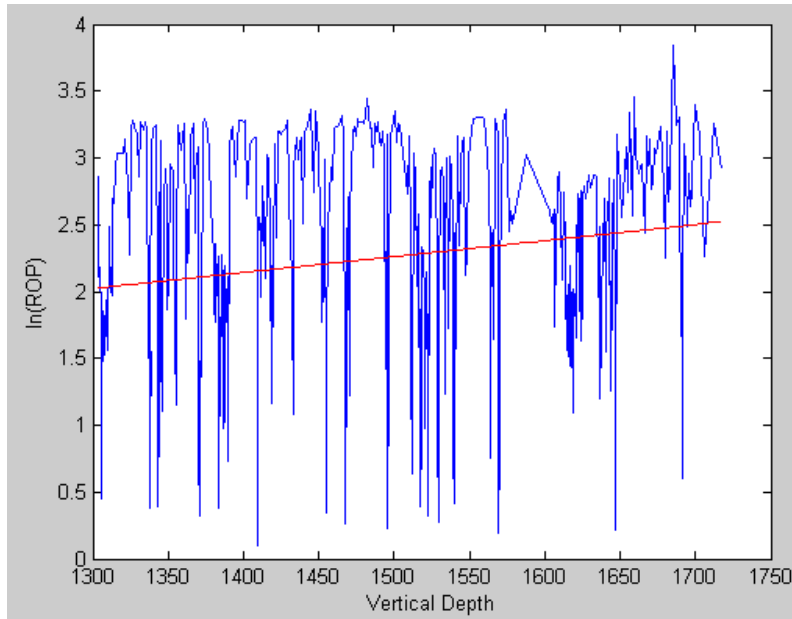
Figure 3-3 Well 0. 17 1/2" bit section. Vertical depth is plotted versus the natural logarithm of ROP. The red line illustrates the trend line characteristic for this plot.

A = 0.0012 in the 17 ½" bit section. A_2 is computed to be equal to -5.210×10^{-4}.

Figure 3-4 shows the 12 ¼" bit section.
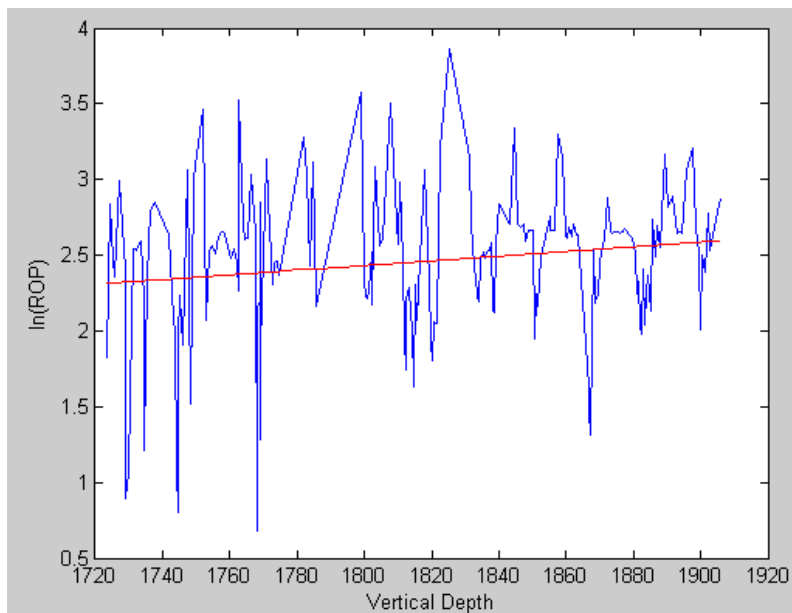
Figure 3-4 Well 0. 12 1/4" bit section. Vertical depth is plotted versus the natural logarithm of ROP. The red line illustrates the trend line characteristic for this plot.

A = 0.0015 in the 12 ¼" bit section. A_2 is found to be equal to -6.513×10^{-4} by using equation 3-11.

Figure 3-5 shows the 8 ½" bit section.
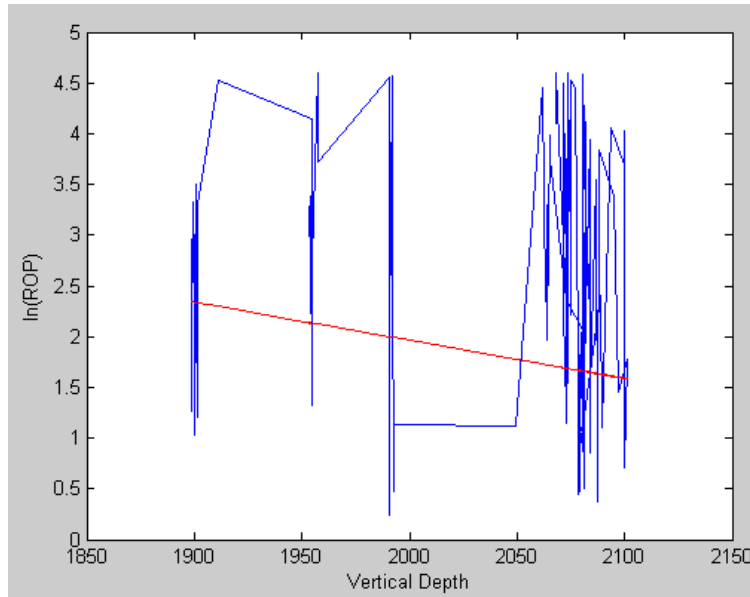
Figure 3-5 Well 0. 8 1/2" section. Vertical depth is plotted versus the natural logarithm of ROP. The red line illustrates the trend line characteristic for this plot. Very little data is available between approximately 1 900 m and 2 050 m.

In the 8 ½" section A = -0.0038. A_2 is estimated to be equal to 1.650×10^{-3} by using equation 3-11.

The rate of penetration tends to decrease with depth mainly due to compaction caused by increasing amount of overlying formations. The depth correction factor is meant to make up for this compaction. To determine the best value of a_2, it is important to consider all four sections in the well. The length and shape of the different sections are shown in Figure 3-6.
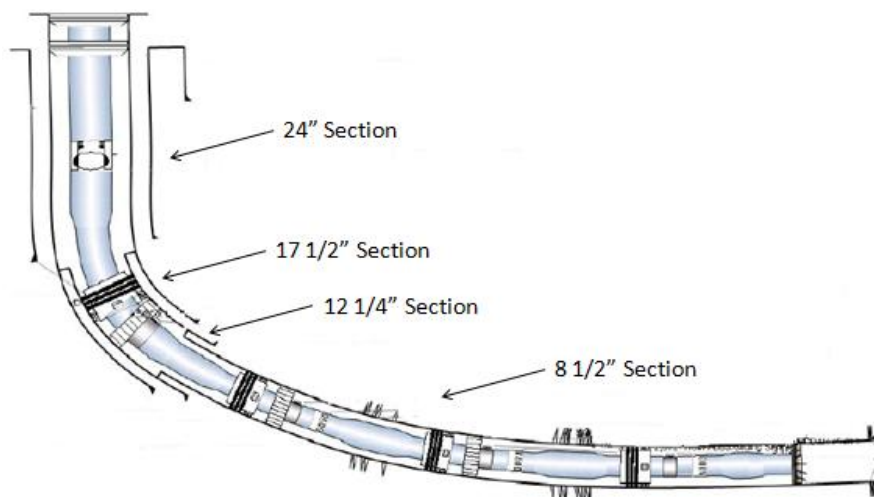

Figure 3-6 Well 0. The length and shape of all four sections (Christophersen, Gjerde and Valdem, 2007).

Some sections are assumed more relevant for the determination of depth correction exponent. In addition to being almost horizontal the 8 1/2" bit section contains very little data (see Figure 3-5). The vertical depth is approximately only 200 m and a reliable trend line is hard to establish. Both the 17 ½" bit section and the 12 ¼" bit section show an increasing trend line. An increasing trend line indicates increased rate of penetration with depth. The 12 1/4" bit section is short (less than 200 m vertical depth). The 17 1/2" bit section is longer, approximately 450 m vertical depth, but still short compared to the 24" section. The vertical length of the 24" bit section is approximately 1 000 m. The 24" bit section was emphasized when determining the compaction exponent. A_2 is in further analyses set to be equal to 10^{-3}.

The weight on bit exponent and the rotary speed exponent are a bit more complex to obtain through linear regression.

Determination of the exponents associated with weight on bit and rotary speed have been proposed by several authors using data relevant of the prevailing conditions. A computerized drilling control system was pioneered by Young (1969), where both weight on bit and rotary speed could be varied systematically with changing formations and the exponents were computed automatically from the observed penetration rate (Bourgoyne, Millhelm and Chenevert et al., 1986). The bit weight exponent obtained from field data, ranges from 0,6 to 2,0. The rotary speed exponent ranges from 0,4 in very hard formations to 0,9 in soft formations (Bourgoyne and Young , 1974).

Both the bit weight exponent and the rotary speed exponent can be obtained by performing a drilloff test. A drill off test is conducted by first selecting a depth with expected uniform lithology. Then lock the break and determine the time required to drill 10% (characteristic time) of the bit weight currently in use. Then increase the bit weight to initial value of the drill off test. The bit weight increase should be at least 20% more than the bit currently in use. Further this bit should be used until a new bottom hole pattern of the bit is established. The time allowed is usually one characteristic time per 10%. Then lock the break again and maintain the current rotary speed. Time should be recorded each time the bit weight falls by 400 lbs. This is continued until only 50% of the initial bit weight is left. Δt vs ΔW and ΔW vs R is then plotted on a log-log paper. The slope of the line is equal to the exponent of the weight on bit. The test is to be repeated for different speeds (Bourgoyne, Millhelm and Chenevert et al., 1986).

The rotary speed exponent can be obtained by using penetration rates at two different rotary speeds with the same bit weight (Bourgoyne, Millhelm and Chenevert et al., 1986). The two penetration rates have to be plotted against average bit weight on a log-log paper. The value of the rotary speed exponent is equal to the distance between the two lines in the parallel region.

4 Testing of model with respect to hardness detection through field data

It may be possible to detect soft and hard formations through real-time drilling data. Statoil has provided real-time data for present master thesis which are completely confidential. The well the data are recorded from is further referred to as Well 0.

4.1 Available data

In addition to real-time drilling data, the FWR for Well 0 has been available. The report contains information about experienced hard stringers. Such information has been used later in this chapter to test the quality of the created program.

All data used during present master thesis are surface recorded data. Of the approximately 60 parameters available from surface data logs, only five have been applied to calculate drillability; WOB, bit RPM, Block Position, bit measured depth and wellbore measured depth (Solberg, 2011).

Downhole recorded real-time data are data transmitted to surface in real time after being recorded. The real-time data are recorded every 5th second, and all data recorded within 24 hours are saved in the same file. The data have to be transferred at an accepted high data rate to become real-time data. The number of data transmitted, or the distance between the measurements, have to be reduced if the data rate is low compared to the drilling or tripping speed. If not, important information may be lost (Schlumberger[4], 2011).

Back to the surface data: They are all recorded every 5th second. The weight applied on the bit is proved to have the highest effect upon the rate of penetration of all mechanical parameters. The penetration rate increases exponentially when adding weight on the bit. Tests have shown that in hard, dense formations, with ROP varying from 5 to 12 ft/h, the penetration rate and weight on bit were often squared proportional. A less increase in ROP vs. WOB appeared in softer formations (Head, 1951).

Rotary speed is measured in rounds per minute and indicates how fast the bit is rotating. The necessity of high rotary speed is lower in harder formations. Cunningham and Goins (1960) found through laboratory drilling tests linear proportionality between rotary speeds and drilling rate in mud at atmospheric pressure. However, under increased differential pressure (hydrostatic-pore), the drilling rate was below linear proportionality (Cunningham and Goins, 1960).

Rate of penetration is determined from the velocity of the block. The penetration rate tends to decrease when entering a harder formation. If the block is moving rapidly, it is most likely due to soft formations. The movement of the block identifies also what part of the drilling operation is being performed. When the block position is increasing, it may indicate that the block is being pulled up to make new connections. If the block position is held constant for a longer period of time, it might be due to performing a connection (Solberg, 2011).

Measured Depth (MD) is the deepest position of the open hole at all time. The bit depth measured is the depth at where the bit appears inside the well. The bit depth and the measured depth are equal while drilling (Solberg, 2011).

4.2 Analyzing field data

Parts of the described analyses below were made by Solberg (2011). As mentioned earlier, the detection of soft and hard formations may be achieved by evaluating real-time drilling data. However, an excellent prediction is impossible to make by only basing the evaluation on one dataset at the time. The datasets need to be compared and seen together with other drilling parameters, e.g. gamma ray, sonic log etc, to be able to predict the strata of the formation if it has not been expressed in the Operational Log in the FWR.

Hard stringers are indicated through BPOS speed (while WOB is fairly constant) several places in the section shown in Figure 4-1.
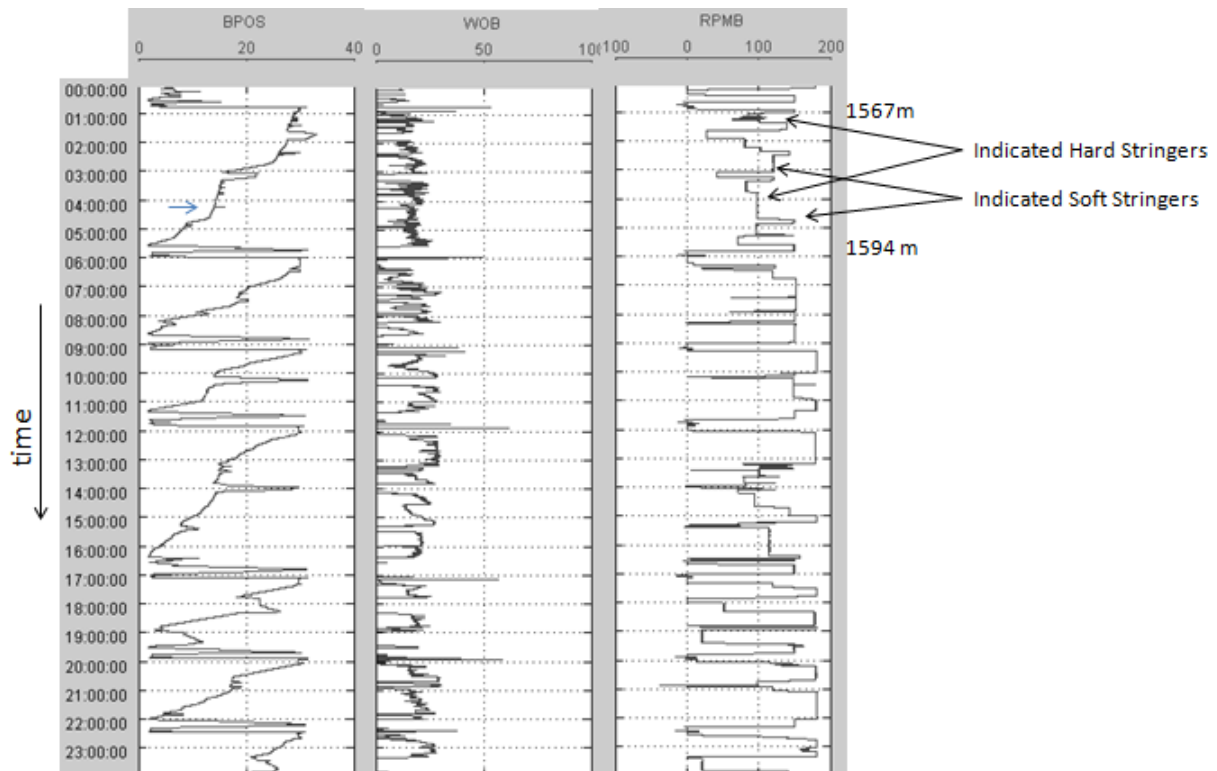
Figure 4-1 Well 0. 17 ½" bit section, interval between 1 560 m and 1 740 m. BPOS, WOB and RPM are plotted vs. time in different real-time drilling windows. Hard stringers are indicated several places in the upper section by low RPM and high WOB (Solberg, 2011).

A decrease in RPM while WOB is increased indicates hard formations. The low velocity of the block in these formations enhances the indications (Solberg, 2011). Figure 4-2 illustrates WOB, RPM and BPOS plotted versus time in the same drilling data window.
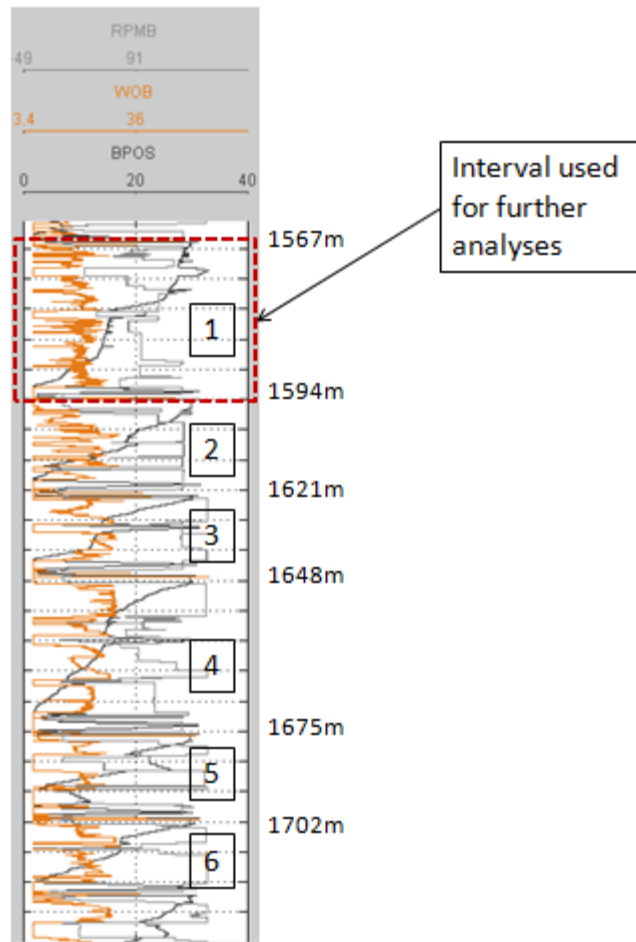
Figure 4-2 Well 0. 17 ½" bit section, interval between 1 560 m and 1 740 m. WOB, RPM and BPOS are plotted vs. time in same real-time drilling window. The interval consists of six block sections (Solberg, 2011).

The block was lowered six times during the section shown in Figure 4-2, indicating that six stands were being drilled. As can be observed, block section 1 and 4 are longer than the other sections. This is due to lower average penetration rates during these intervals compared to interval 2, 3, 5 and 6. Lower penetration rate is most likely caused by harder formations. Block section 1 will be utilized for further analyses in this chapter due to existence of both hard and soft formations during this interval (Solberg, 2011). See Figure 4-3.
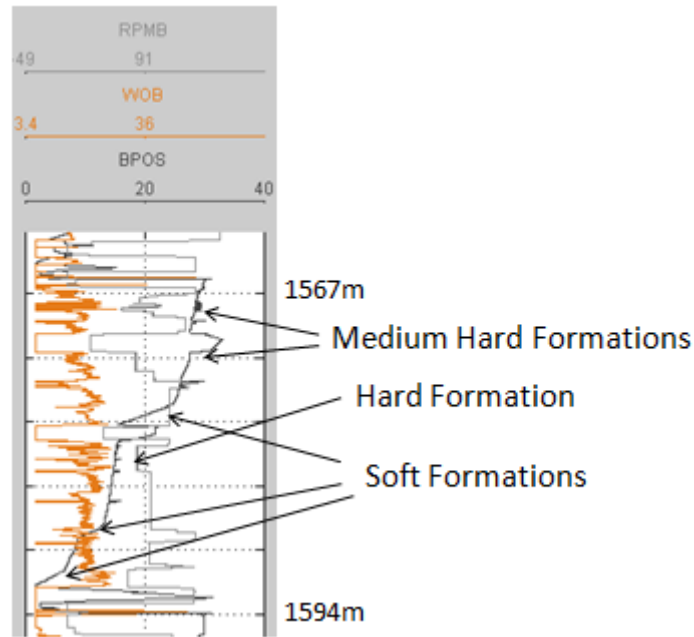
Figure 4-3 Well 0. 17 ½" bit section, interval 1 560 m to 1 595 m. WOB, RPM and BPOS are plotted vs. time. Both hard formations (low RPM, high WOB and slow movement of the block) and soft formations (high RPM, low WOB and fast movement of the block) are indicated.

The interval between 1 560 m and 1 595 m contains both hard and soft formations. Soft formations are indicated by high RPM and relatively low WOB.

ROP is estimated by the data service company. However, it is preferable to apply raw data and manipulate the data in controlled manner. The derivative of the block position with regard to time (ΔBPOS/Δt) has been computed and is equal to the velocity of the block. The derivative of block position (BPOS) with regard to time will be further referred to as ΔBPOS. ROP (from data provider) and ΔBPOS are plotted versus measured depth in Figure 4-4 (Solberg, 2011).
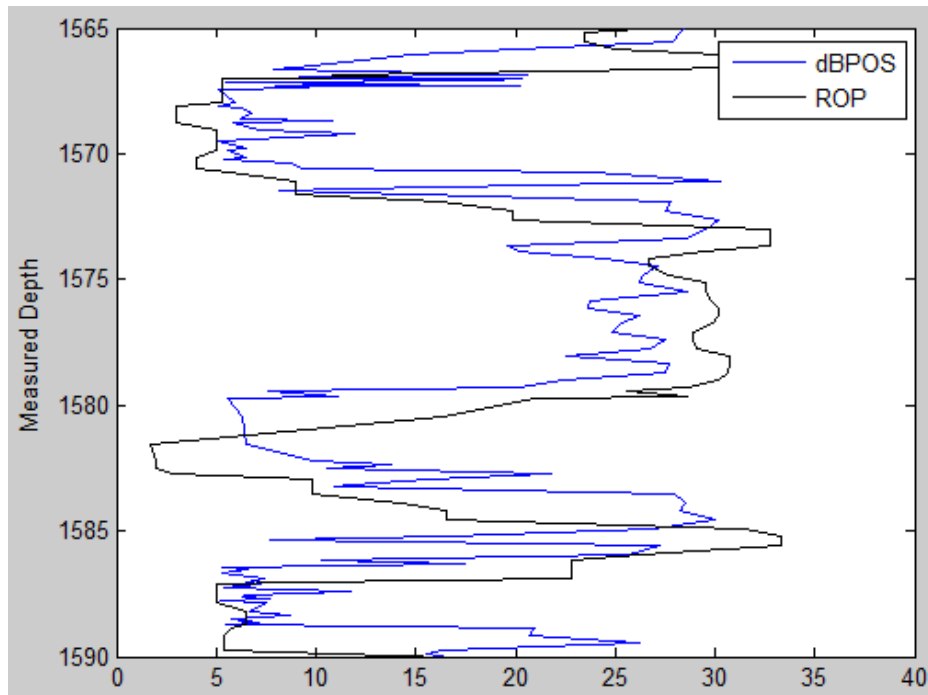
Figure 4-4 Well 0. ΔBPOS and ROP are plotted vs. measured depth (m). ΔBPOS is computed based on BPOS

From Figure 4-4 it can be seen that ROP and ΔBPOS show the same trend and to some degree the same values. However, by using ROP in further calculations of drillability, the hardness in the formation will not correspond with the correct depth. The hard formations will be estimated deeper than where they actually are situated when using ROP. ΔBPOS will be further utilized in calculations of drillability and hardness.

4.3 The program

To achieve an automatic detection of hardness from real-time data, a Matlab program has been created. The program was started on by Solberg (2011) and improvements and modifications have been applied during present master thesis. The program computes drillability using the simplified equation by Bourgoyne and Young (1986) (Equation 3-6). The program imports seven different parameters from real-time drilling data which are time, vertical depth, measured bit depth, measured depth, weight on bit, block position and rotary speed. The program consists primarily of executing functions and the main executions are described in Figure 4-5 by a flow chart. The Matlab codes are attached in Appendix I.

Start

Write All Filenames In A List

Read Next Filename

Is The Current Operation Drilling?
Is DMEA(1) =/ DMEA(end) ?

No

Yes

Eliminate Odd Values

Sort Rows DMEA(i) < DMEA(i+1)

Compute Average of Several Data Points of All Datasets

Compute dBPOS

Calculate Max Drillability

Calculate Drillability/ Hardness

Compute Average Drillabilities of Several Points

Normalize Hardness by Dividing by Max Hardness

Plot Hardness

End

Figure 4-5 Flow chart of the program made to compute hardness in the formation. It consists mainly of executing functions.

The main program reads files containing real-time data. However, some files contain only data recorded during other operations than drilling (tripping in/out, change of bit size etc). To eliminate the files that do not contain relevant drilling information, the first and the last measured depths (DMEA) in the files are read and compared.

For example; DMEA(1) is the first depth recorded in the file. DMEA(n) is the last depth recorded in the file. If DMEA(1) == DMEA(n), then no drilling has occurred during the interval and the file is eliminated. If DMEA(1) =/ DMEA(n), the file is saved.

This is checked for in every file before continuing the executions. For the files that contain drilling data, all relevant initial lists of data (RPM, WOB, BPOS, DMEA, DBTM, DVER and time) are read and saved together with data from the other drilling files.

The three first functions eliminate odd values of RPM, WOB and DMEA. RPM is set to rotate at least 25 rounds per minute and all RPM parameters lower than 25 are removed. WOB is set to be larger than 2.5 ton meaning that values of WOB less than 2.5 ton are not taken into consideration when calculating drillability.

To make sure that the data comes in correct order, the data are sorted with respect to measured depth. Averages of several data points in each dataset are computed (3, 9 or 27 points at a time) due to huge amount of data in short time intervals.

Equation 4-1 illustrates the average computation of block position of three points.

$$BPOS(i) = \frac{BPOS(i-2) + BPOS(i-1) + BPOS(i)}{3} \qquad (4\text{-}1)$$

The next function computes the speed of the block which should be equal to the drilling rate (ROP). This is done by computing the slope between two block positions using Equation 4-2.

$$dBPOS(i) = \frac{BPOS\_average(i-1) - BPOS\_average(i)}{15} \, x \, 3600 \qquad (4\text{-}2)$$

If the average of three block positions was computed, there would be 15 seconds between each average block position. The equation is multiplied by 3 600 to achieve the correct units to be able to compare ΔBPOS and ROP (Figure 4-4).

The velocity of the block is set to range between 1.5m/h and 30.5 m/h and. Block velocity values out of this range is eliminated in the next function.

The next function determines the drillability along the complete section. It estimates the maximum drillability by applying only one WOB exponent and one RPM exponent. The largest drillability is essential to be able to normalize and define the drillability values in hard and soft formations. Equation 4-3 illustrates the execution of the normalization which is executed in another function,

$$Normalized\ Drillability(i) = \frac{Drillability(i)}{Max\ Drillability} \qquad (4\text{-}3)$$

The calculation in equation 4-3 makes the drillability range from 0 to 1. In present work, drillabilities < 0.5 are assumed to be calculated from hard formations. The normalization makes it possible to apply more than one WOB exponent and one RPM exponent.

The next function calculates the drillability by considering two different exponents for each exponent type (WOB and RPM). One exponent of each exponent type is related to harder formations while one exponent of each exponent type is related to softer formations. The hardness is then calculated by using Equation 2-1 from chapter 2.3.

$$Hardness = \frac{1}{Drillability} = \frac{1}{K} \qquad (2\text{-}1)$$

The maximum hardness along the complete section is determined and the hardness is normalized by using hardness instead of drillability in Equation 4-3.

To achieve a smoother curve when plotting large depth intervals, averages of hardness may be computed.

4.4 Hardness result

The improved and modified program presented in chapter 4.3 has been tested by utilizing data from Well 0. Unfortunately, data from other wells were not available during present master thesis.

The well consists of four sections, the 24", 17 ½", 12 ¼" and 8 ½" bit section. Data from the 17 ½" bit section between 1 565 m and 1 590 m have been applied due to existing information in this area. As mentioned previously, hard stringers were experienced in some parts of this interval according to FWR.

Making hardness detection as accurate as possible is a stepwise approach and consists of elimination of odd data, normalization of drillability/hardness and applying exponents for both hard and soft formations.

Hardness calculated from all raw data has been plotted in Figure 4-6.
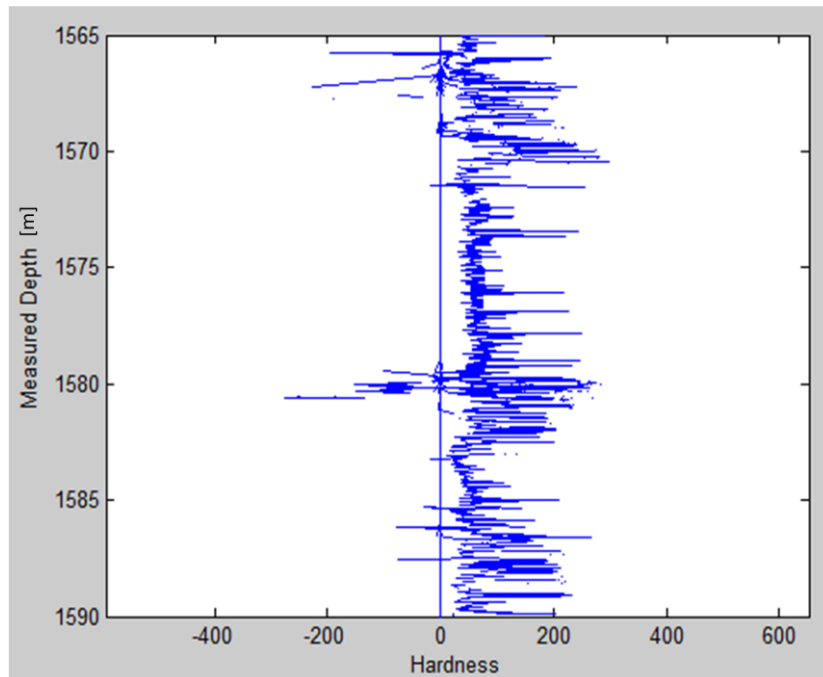
Figure 4-6 Well 0. Interval 1 565m to 1 590 m. Hardness is plotted vs. measured depth (m). All raw data have been utilized to calculate hardness including negative values.

When plotting hardness against measured depth, some negative hardness values appear. These negative hardness values are not logical and need to be removed. In addition to eliminating odd data, several other modifications are necessary to improve the readability of the plot. Following stepwise modifications are made and illustrated further in this chapter:

1. Elimination of odd data
2. Normalization of hardness by computing average of nine points (possible to alter)
3. Further normalization to make hardness range from 0 to 1
4. Applying two exponents for both WOB and RPM exponents
5. Changing definition of drillability in hard formations

Eliminations of unlikely high and low values of RPM, WOB and ΔBPOS have been made to avoid wrong drillability and hardness values and to improve the readability of the plot. Figure 4-7 shows the hardness plot when such eliminations have been applied.
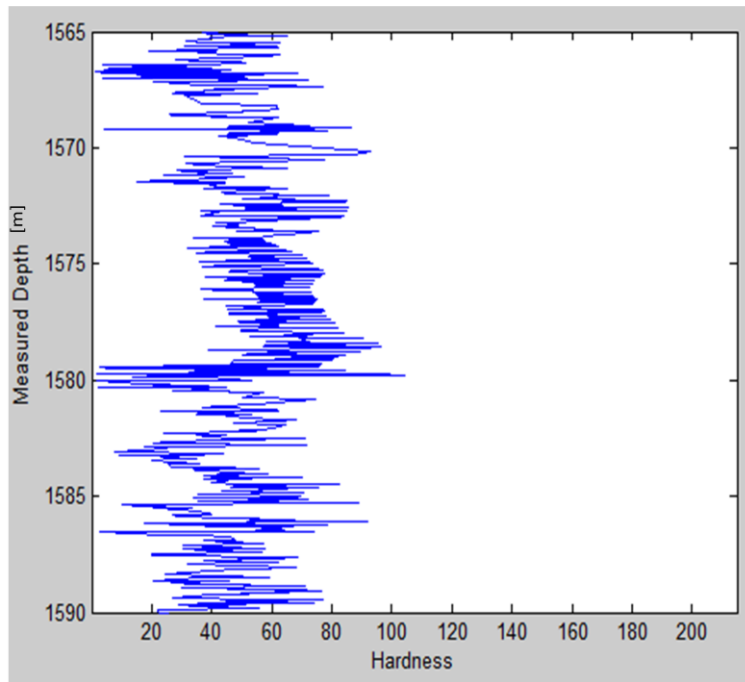
Figure 4-7 Well 0. Interval 1 565 m to 1 590 m. Hardness is plotted vs. measured depth (m). Uninteresting values of RPM, WOB and ΔBPOS have been removed (modification #1).

The negative hardness values are eliminated and the readability of the plot is improved in Figure 4-7 compared to Figure 4-6.

The plot may be normalized by computing the average of several hardness points at the time. The normalization is illustrated in Figure 4-8 where the average of nine points is computed.
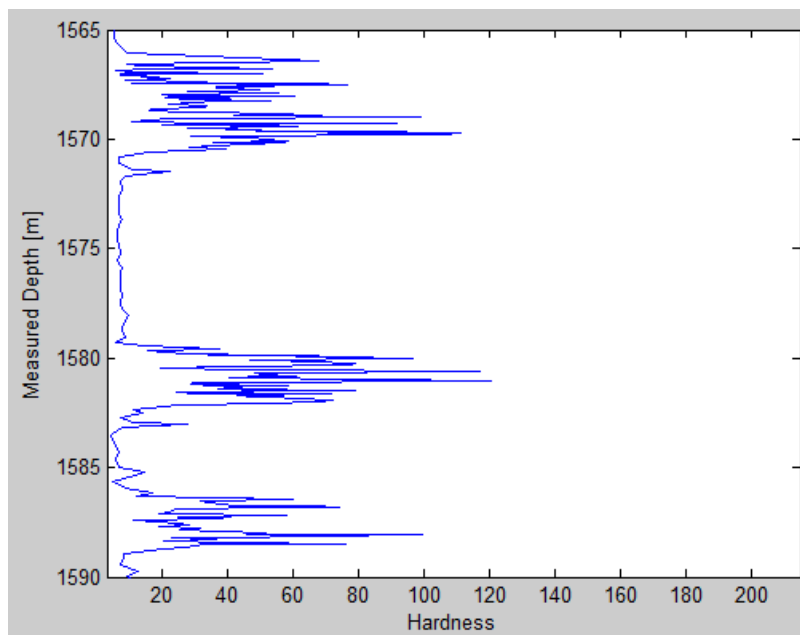

Figure 4-8 Well 0. Interval 1 565m to 1 590 m. Hardness is plotted vs. measured depth (m). The average of nine hardness points has been computed to normalize the plot (modification #2).

The normalization makes the plot smoother and better to read.

As the correct values of drillability and hardness are insignificant in present work, the hardness is set to range from 0.0 to 1.0, where 1.0 indicates extremely hard formations. The scaling of hardness also makes it easier to compare the hardness values within the plot. Scaling has been executed in Figure 4-9. Figure 4-8 and Figure 4-9 look similar except from the values on the x-axis.
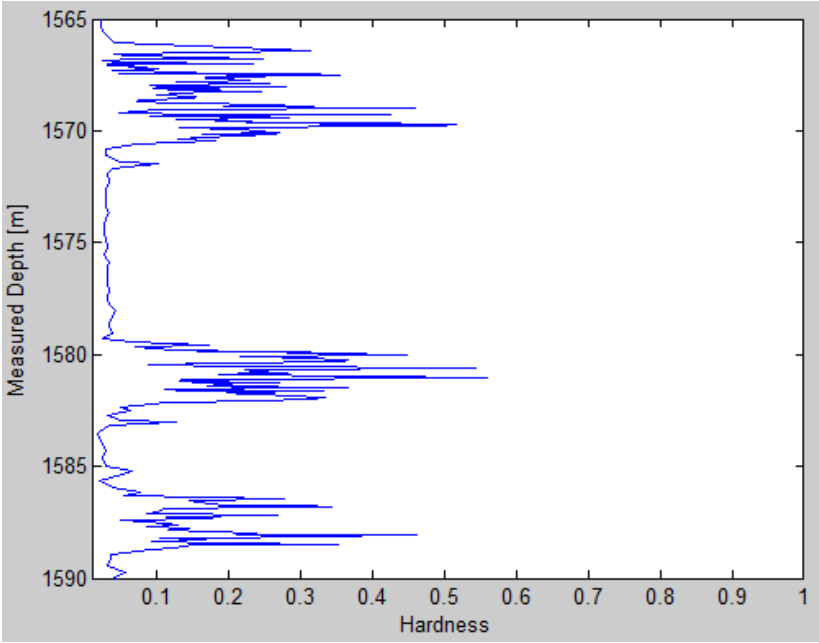

Figure 4-9 Well 0. Interval 1 565m to 1 590 m. Hardness is plotted vs. measured depth (m). Further normalization has been applied to make the hardness range from 0 to 1 (modification #3).

The calculations of drillability and hardness illustrated in Figure 4-6 to Figure 4-9 have been executed by utilizing only one exponent value for each exponent type, which were exponents related to medium soft and medium hard formations. In Figure 4-10, exponents related to harder formations are applied.
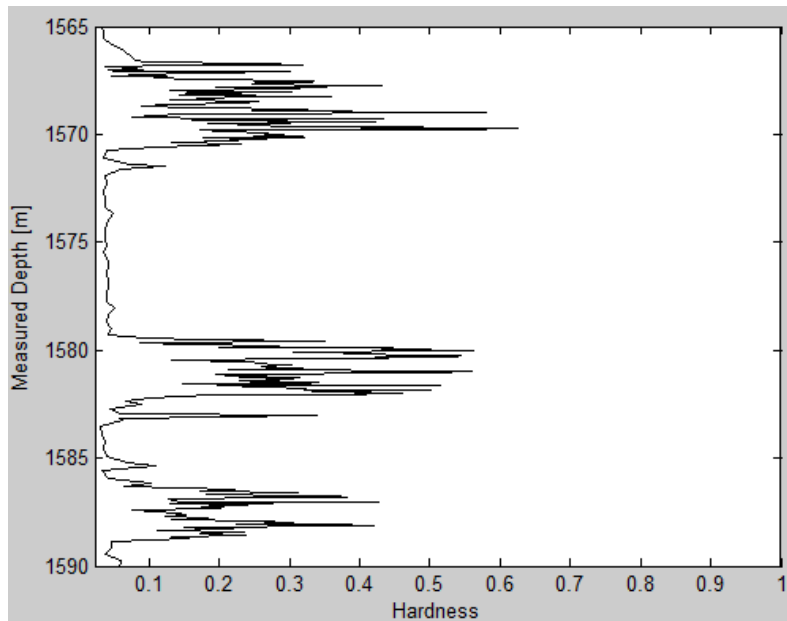
Figure 4-10 Well 0. Interval 1 565m to 1 590 m. Hardness is plotted vs. measured depth (m). Two exponents of both RPM and WOB have been applied. In soft formations moderate soft formation exponents are applied. In hard formations extremely hard formation exponents are applied (modification #4).

In Figure 4-10, moderate soft formation exponents (a5 = 1.5 and a6 = 0.8) have been applied in soft formations and extremely hard formation exponents (a5 = 0.6 and a6 = 0.4) have been applied in harder formations. Figure 4-11 illustrates hardness when exponents related to softer formations are applied.
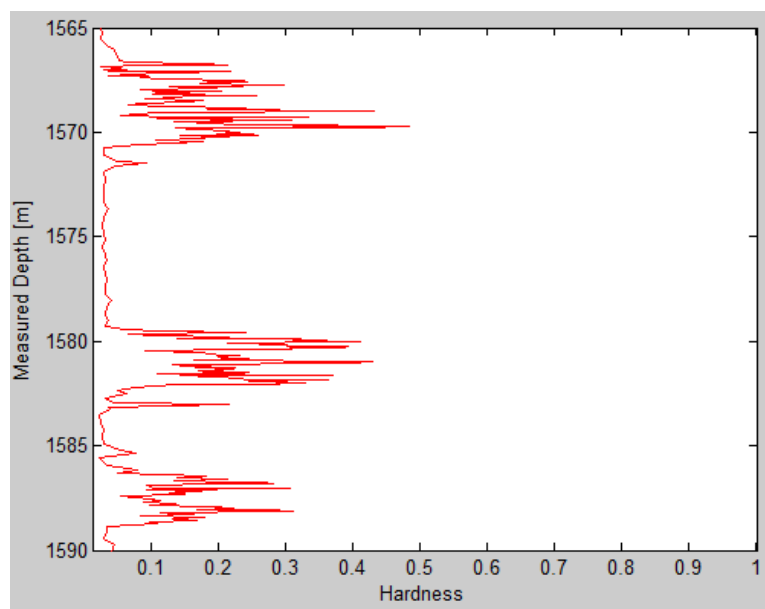

Figure 4-11 Well 0. Interval 1 565m to 1 590 m. Hardness is plotted vs. measured depth (m). Two exponents of both RPM and WOB have been applied. In soft formations extremely soft formation exponents are applied. In hard formations moderate hard formation exponents are applied (modification #4).

Figure 4-11 illustrates when extremely soft formation exponents (a5 = 2.0 and a6 = 0.9) have been applied in soft formations and moderate hard formation exponents (a5 = 0.9 and a6 = 0.6) have been applied in harder formations.

The difference between using different exponent values (the difference between Figure 4-10 and Figure 4-11) is illustrated in Figure 4-122.
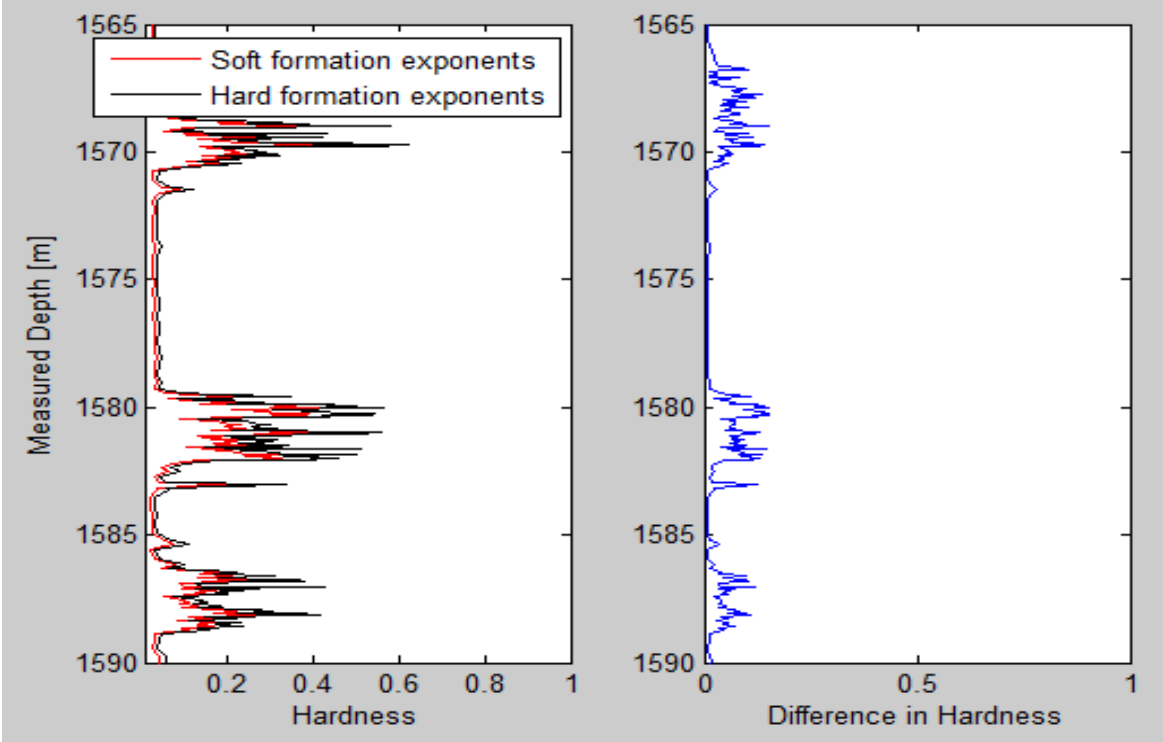

Figure 4-12 Well 0. Interval 1 565m to 1 590 m. Left window: Hardness vs measured depth(m). The black curve illustrates hardness when exponents related to harder formations are applied. The red curve illustrates hardness when exponents related to softer formations are applied. Right window: The difference in hardness between the two curves illustrated in the left window (modification #4).

The right window in Figure 4-12 shows the difference between the two hardness curves seen in the left window. Calculations of hardness when using exponents related to harder formations show larger variation in hardness compared to when softer formation exponents are applied. Exponents related to harder formations are used in further analyses.

To be able to apply two different exponents for both WOB and RPM, the values of drillability have to be divided into two categories. The drillabilities of lower values than 0.5 were classified to be calculated as hard formations and the rest as soft formations. In Figure 4-13, the drillability definition in hard formations is reduced to below 0.3.
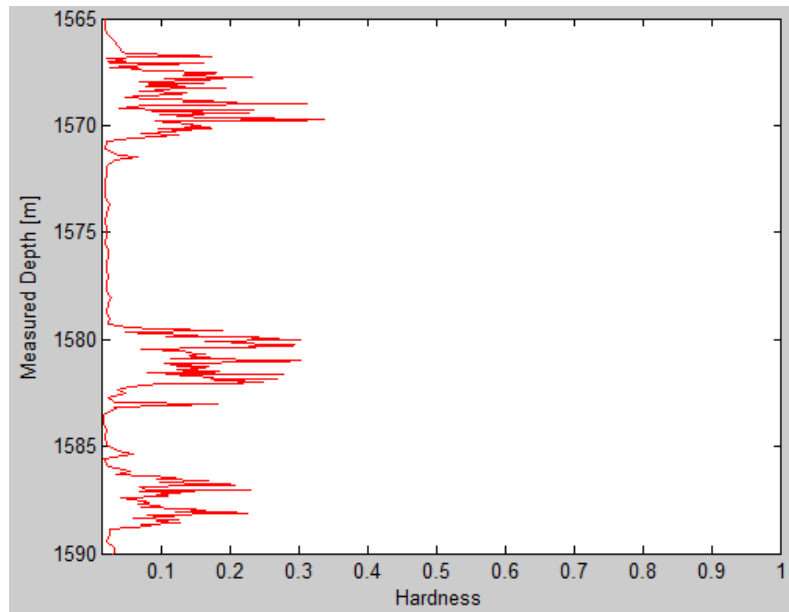
Figure 4-13 Well 0. Interval 1 565m to 1 590 m. Hardness is plotted vs. measured depth (m). The definition of hard formations is reduced to drillabilities < 0.3 (modification #5).

Altering the definition of hard formation drillability from less than 0.5 to less than 0.3 affects the hardness plot. The difference between the two definitions is seen in Figure 4-14.
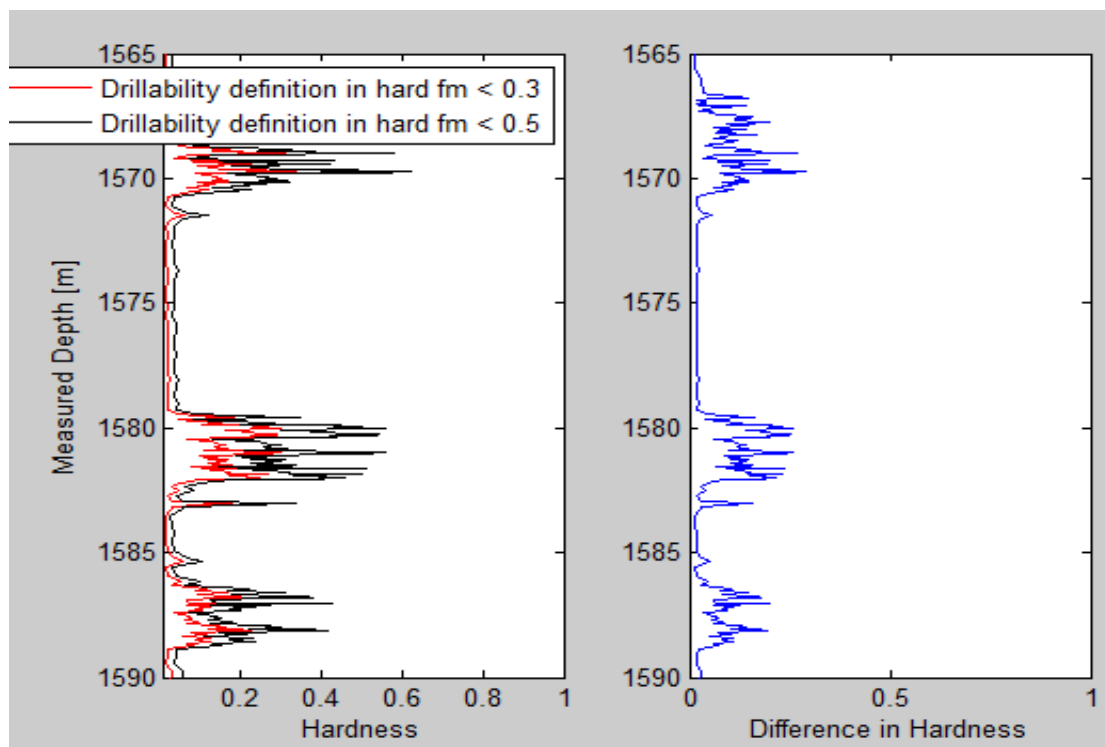
*Figure 4-14 Well 0. Interval 1 565m to 1 590 m. Left window: Hardness is plotted vs. measured depth (m). the black curve illustrates hardness when the drillability definition of hard formations < 0.5 and the red curve illustrates hardness when the drillability definition of hard formations < 0.3. Right window: The difference between the two curves illustrated in the left window is shown (modification #5).*

The right window in Figure 4-14 shows the difference between the two hardness curves seen in the left window. The definition of drillability in hard formations < 0.5 has more distinct transitions and is being applied for the final result.

According to FWR, hard stringers were experienced in the 17 ½" bit size section between 1 556 m and 1 587m. Hard stringers may be indicated at least three places in the interval between 1 556 m and 1 587 m (Solberg, 2011). This was illustrated previous in Figure 4-1. The indication is based on looking at RPM, WOB and ΔBPOS together. Decrease in RPM together with an increase in WOB indicates hard formations. Figure 4-15 shows a cut of only the experienced hard stringer interval from Figure 4-1.
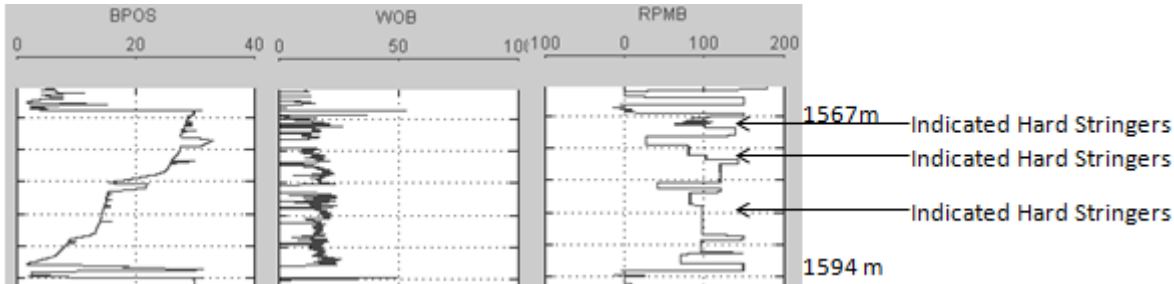

Figure 4-15 Well 0. Interval 1 565m to 1 590 m. Hard stringers were indicated at least three different places during this interval. The indication is based on low RPM followed by an increase in WOB (Solberg, 2011).

Intervals with little change in BPOS with time result in steep curves. Such steep curve intervals denote that the velocity of the block is low and may indicate hard stringers (Solberg, 2011). In addition to low RPM and high WOB, the speed of the block position is also indicating the hard stringers pointed out in Figure 4-15. The computed ΔBPOS is plotted in the same window as BPOS in Figure 4-16 and illustrates the relation between the velocity of the block and the abruptness of the BPOS curve.
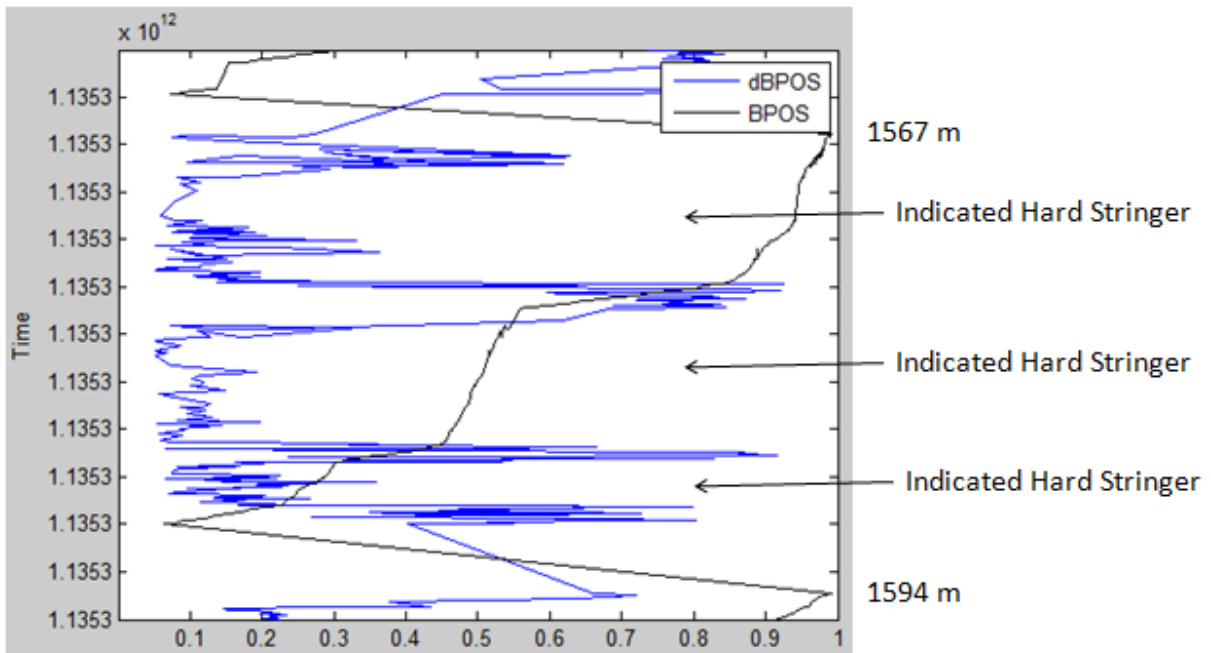
*Figure 4-16 Well 0. Interval 1 565m to 1 590 m. BPOS and ΔBPOS are plotted vs. time. Hard stringers are indicated by low velocity (ΔBPOS) and steep curve of BPOS.*

As can be observed from Figure 4-16, low velocity appears where hard stringers have been indicated by RPM and WOB in Figure 4-15.

The hard stringers indicated by RPM, WOB, ΔBPOS and BPOS are also recognized in the hardness plot in Figure 4-17.
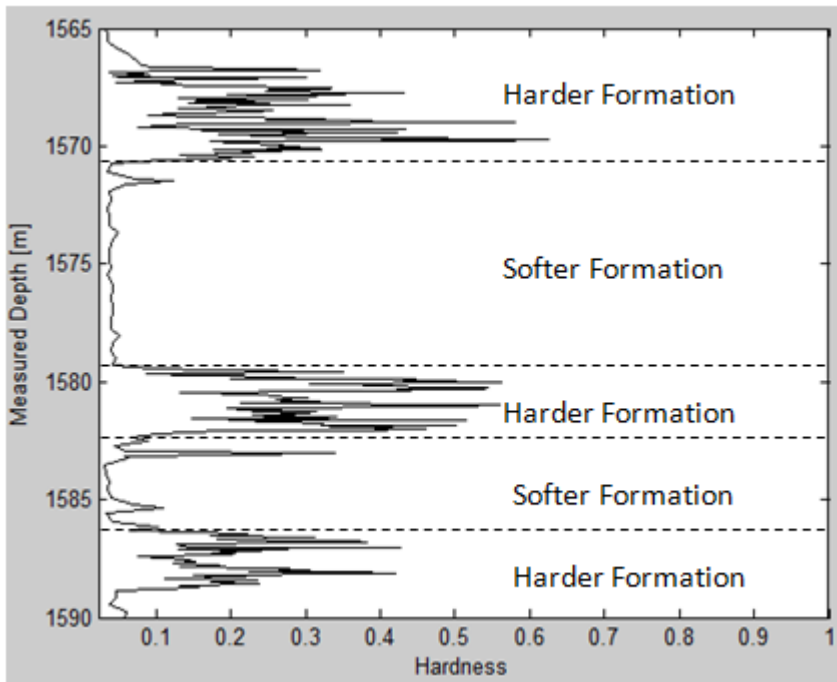
Figure 4-17 Hardness is plotted versus measured depth (m). Hard stringers are indicated by the hardness plot between 1 565 m and 1 590 m.

Figure 4-18 illustrates indications of hard and soft formations by both hardness and ΔBPOS plotted vs. measured depth.
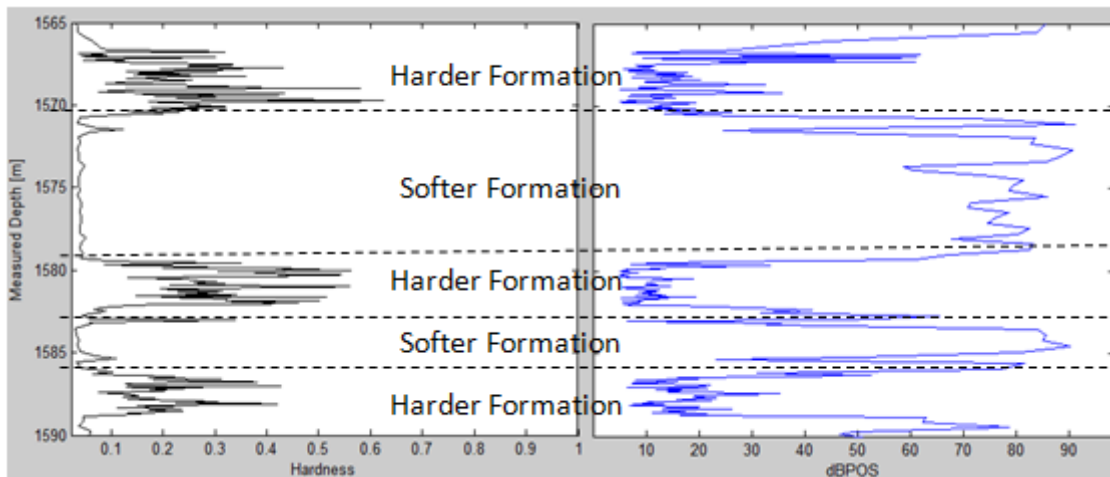
Figure 4-18 Well 0. Interval 1 565m to 1 590 m. Hardness (left) and ΔBPOS (right) are plotted versus measured depth (m) Hard stringers are indicated by hardness and ΔBPOS during this interval.

4.5   Analyzing the impact of the determined depth correction factor on hardness

The previous determined depth correction factor`s impact on hardness has been tested for the 24" bit and the 17 1/2" bit sections due to most relevant data from these sections.

The depth correction factor corrects for an increase in hardness due to compaction with depth. Figure 4-19 illustrates hardness in 24" bit section with and without applying the determined correction factor.
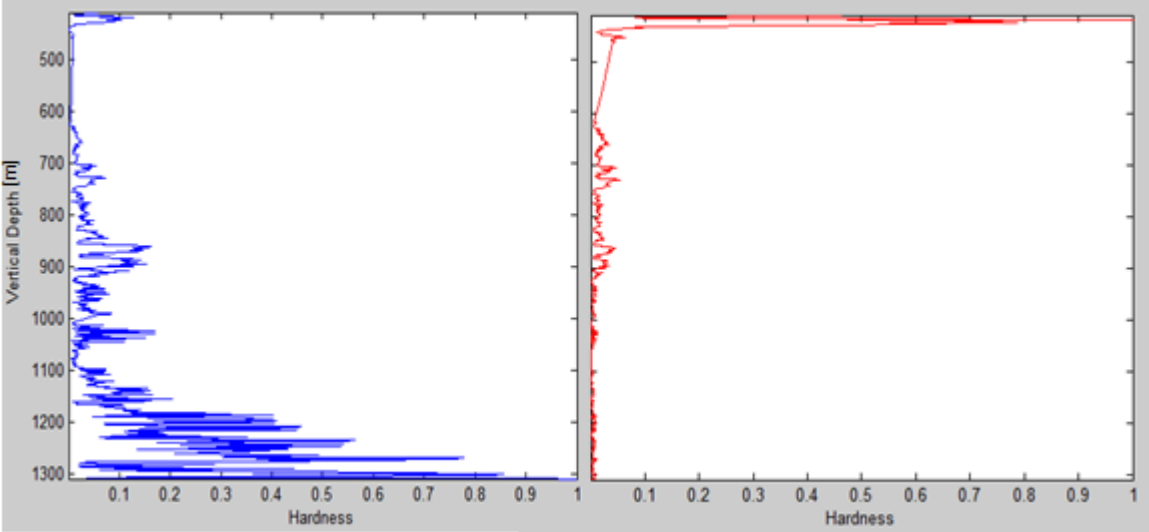
Figure 4-19 Well 0. 24'' bit section, 0 m to 1 393 m. Hardness is plotted versus vertical depth (m). Left window: Hardness without depth correction factor. Right window: Hardness with depth correction factor (a2 = 0.001) applied.

As can be observed from Figure 4-19, the hardness rather decreases with depth than increases when applying the depth correction factor. This may be due to too large correction exponent that was determined in chapter 3.2.2. A lower exponent value is applied in the right window in Figure 4-20.
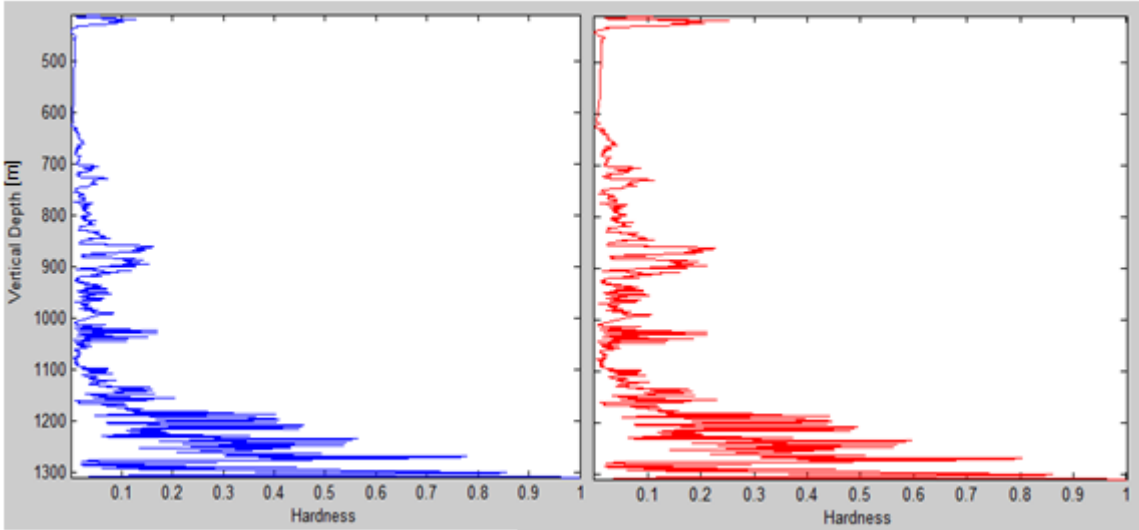

Figure 4-20 Well 0. 24'' bit section, 0 m to 1 393 m. Hardness is plotted versus vertical depth (m). Left window: Hardness without depth correction factor. Right window: Hardness with depth correction factor (a2 = 0.0001) applied.

When the depth correction exponent is lowered by a tenth the hardness values are increased in some intervals. However, the increased hardness in some intervals does not affect the transition between the harder and softer formations which is of interest in present work.

Figure 4-21 illustrates hardness with and without depth correction applied in the 17 1/2" bit section.
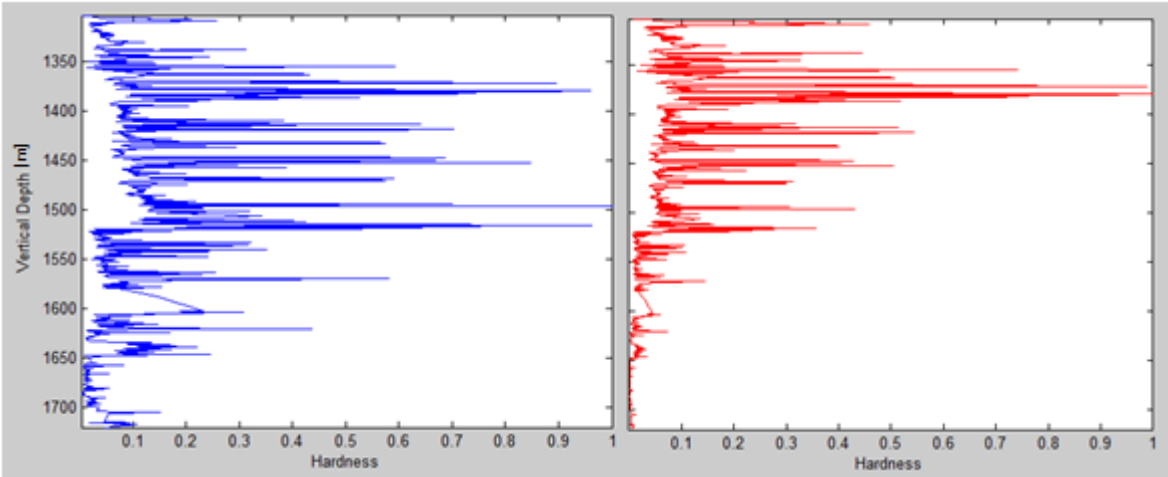
Figure 4-21 Well 0. 17 1/2" bit section, 1 393m - 1 721m. Hardness is plotted versus vertical depth (m). Left window: Hardness without depth correction factor. Right window: Hardness with depth correction factor (a2 = 0.001) applied.

The same trend is seen in the 17 1/2" bit section as in the 24" bit section when applying the depth correction factor applied.

The depth correction exponent is lowered by a tenth in Figure 4-22.
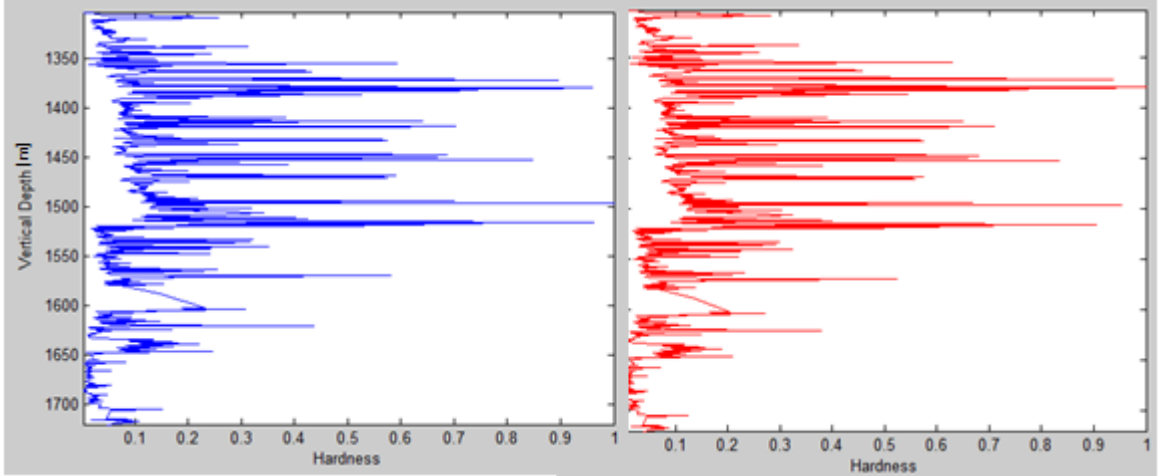
Figure 4-22 Well 0. 17 1/2" bit section, 1 393m - 1 721m. Hardness is plotted versus vertical depth (m). Left window: Hardness without depth correction factor. Right window: Hardness with depth correction factor (a2 = 0.0001) applied.

There is almost no change in hardness due to applying a lower depth correction factor. The depth correction exponent has not been applied in further analyses. Drillability equation 3-6 is then reduced to the equation below;

$$K = \frac{ROP}{(W)^{a_5} x\ (N\ )^{a_6}}$$

(4-4)

5 Comparing hardness with lithology

When drilling a well, the bit drills through different formations. A formation is defined as a series of rocks with certain characteristics in common (The Free Dictionary, 2012). This chapter will evaluate the change in hardness due to entering new formations and the possibility of determining the lithology type by looking at the hardness curve.

The formations drilled in Well 0 are well known formations in the North Sea. Figure 5-1 describes their position in Well 0.

Formation	Measured Depth [m RKB]	True Vertical Depth [m MSL]	TVD deviation from prognosis
Top Utsira Fm.	995	882	+4
Top sandy Hordaland	1050	927	
Top sandfree Hordaland	1655	1282	
Top Balder Fm.	2050	1486	-1
Top Lista Fm.	2200	1555	
Top Shetland Gp.	2411	1655	-6

Figure 5-1 Well 0. Formation tops with depth and deviation from the prognosis (Christophersen, Gjerde and Valdem, 2007).

The formation tops are further illustrated in Figure 5-2.
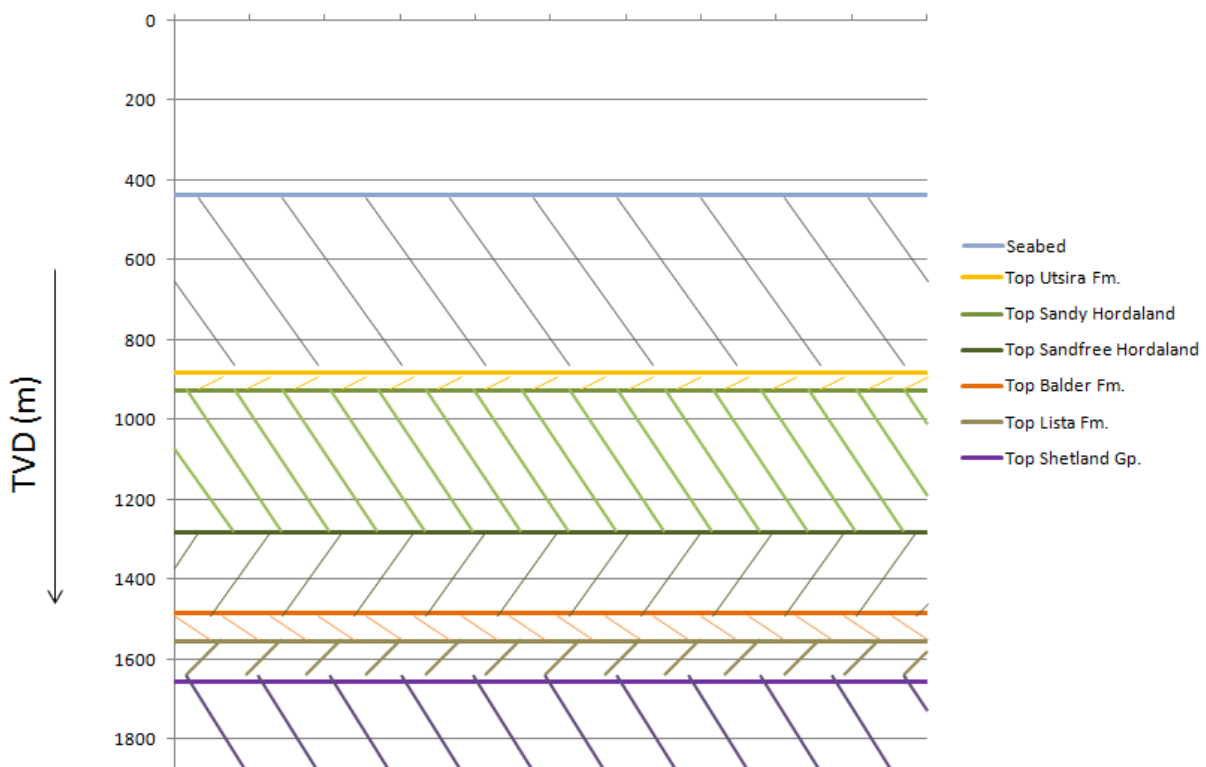

Figure 5-2 Well 0. The formation tops (in m TVD) from all sections drilled in Well 0.

5.1   Formation descriptions

According to FWR Well 0 consists of the Utsira Fm, sandy and sandfree Hordaland, Balder Fm, Lista Fm and the Shetland Group. Not much research has been done on the mentioned formations compared to for instance Brent Fm. The Utsira Fm has very limited log-coverage due to the desire of placing a 20" casing through the formation, and often the sonic and density logs are missing. The other formations mentioned above have larger log-coverage, especially Balder Fm and Lista Fm (Personal comments: Graue, 2012).   The different formations are further described below.

The Utsira formation consists of highly porous (35%-40%) and extremely permeable sands which are organized into approximately 30 m thick packages. The packages are being separated by thin, low-permeability shale layers. These shale layers are assumed to contain potential fluid pathways of erosive deformational origin (Zweigel, Arts and Lothe et al., 2012).

The Hordaland group consists of marine claystones with minor sandstones. Thin limestones and streaks of dolomite appear. The sandstones are normally very fine to medium grained and are often interbedded with claystones. The sandstones are developed at various levels in the group (NPD fact pages[1], 2012). The Hordaland group is divided into sandy and sandfree Hordaland in Well 0.

In the North Sea, the Rogaland group is subdivided into twelve formations (NPD fact pages[2], 2012). However, only two of these are indicated or present in Well 0, Balder and Lista Fm.

The Balder Formation consists of thin layers of varicoloured, fissile shales with interbedded sandy tuffs and occasional stringers of limestone, dolomite and siderite (NPD fact pages[3], 2012)

The Lista Formation consists of brown to grey-brown shales, which are normally non-tuffaceous and poorly laminated. The formation may contain stringers of limestone, dolomite and pyrite and locally thin sandstone layers (NPD fact pages[4]. 2012).

The Shetland Group consists of chalk facies of the chalky limestones, limestones, marls and calcareous shales and mudstones. Chert (flint) exists throughout the facies. The siliciclastic facies consists of mudstones and shales, partly interbedded with limestones. Some sandstones may also be present in the lower part. The shales and sandstones alter from slightly to very calcareous (NPD fact pages[5]. 2012).

5.2 The change in hardness of shale (and sand) due to heat, pressure and chemical reactions

Shale is a sedimentary rock and the sediments are divided by particle sizes into gravel, sand, silt and clay. Claystones consist mainly of clay. The presence of fissility, the property of rocks to split along planes of weakness into thin sheets, makes claystone shale (About.com, 2012a). After deposition, a rock is exposed to weathering, then diagenesis and later metamorphism. Weathering occurs at the earth`s surface. All other physical and chemical changes in sediments after deposition are called diagenesis. The boundary between diagenesis and metamorphism is arbitrary. Diagenesis is sometimes referred to as "burial metamorphism" and for practical purposes; the maximum temperature of diagenesis can be set to approximately 300°C (Eslinger and Peaver, 1988). At this temperature, clay minerals have been transformed to mica and chlorite of the greenschist facies. The main physical change during shale diagenesis is compaction, which drives out pore water. The porosity of shale may decrease from approximately 70-90% to 30-35% due to overlying formations. Further, the porosity may continue decreasing, but now due to that the adsorbed water is being driven out or that the clay minerals is being deformed or recrystallyzed. In comparison, the porosity of sand decreases from 40% to 25-30% due to compaction. The sand porosity may decrease to approximately 15% if sufficient amount of small grains is present (Prestvik, 2001). These small grains will occupy normally empty pore spaces. The compaction due to the escape of water is generally completed by burial to approximately 3000 ft (ca 915 m) (Eslinger and Peaver, 1988). Shale can be fairly hard if it contains silica cement. The rock slate is derived from shale by regional metamorphism which happens when shale undergoes great heat and pressure (About.com.geology, 2012b). During metamorphism clay begins to revert to mica minerals, which is a group of silicate minerals (About.com, 2012c). Figure 5-3 shows hypothetical curves of the change of hardness of shale and sand versus depth. The curves are based on the processes mentioned above. The compaction of sand with depth is assumed to be not as affected as shale.
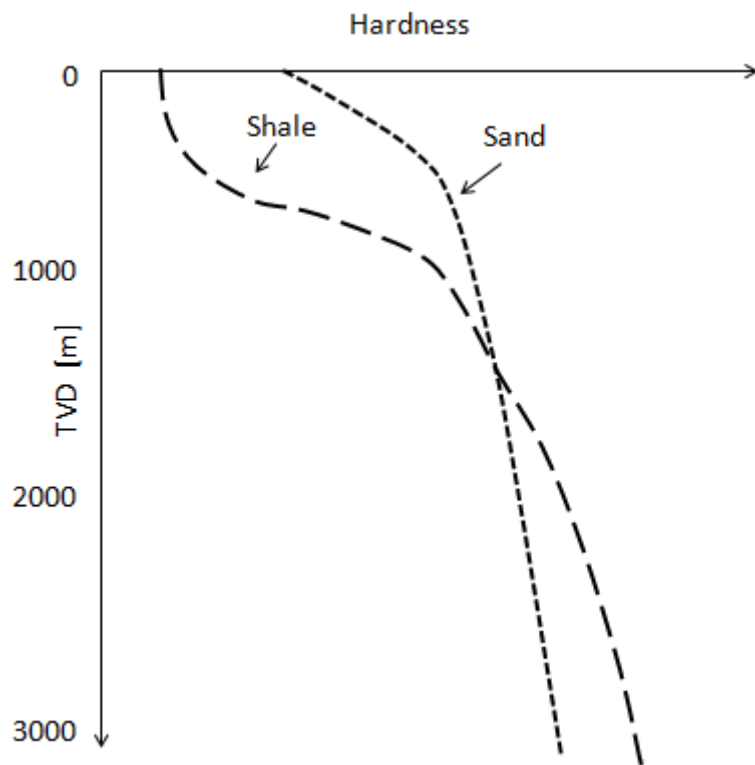
Figure 5-3 Hypothetical shale hardness and sand hardness is plotted vs vertical depth.

5.3 Analyzing hardness as an indicator of lithology determination

The same data and hardness curves used in hardness detection in chapter 4.4 are utilized for lithology detection.

The 24" bit section consists mainly of two formations, Utsira Fm and sandy Hordaland Fm. Figure 5-4 illustrates the hardness in this section.
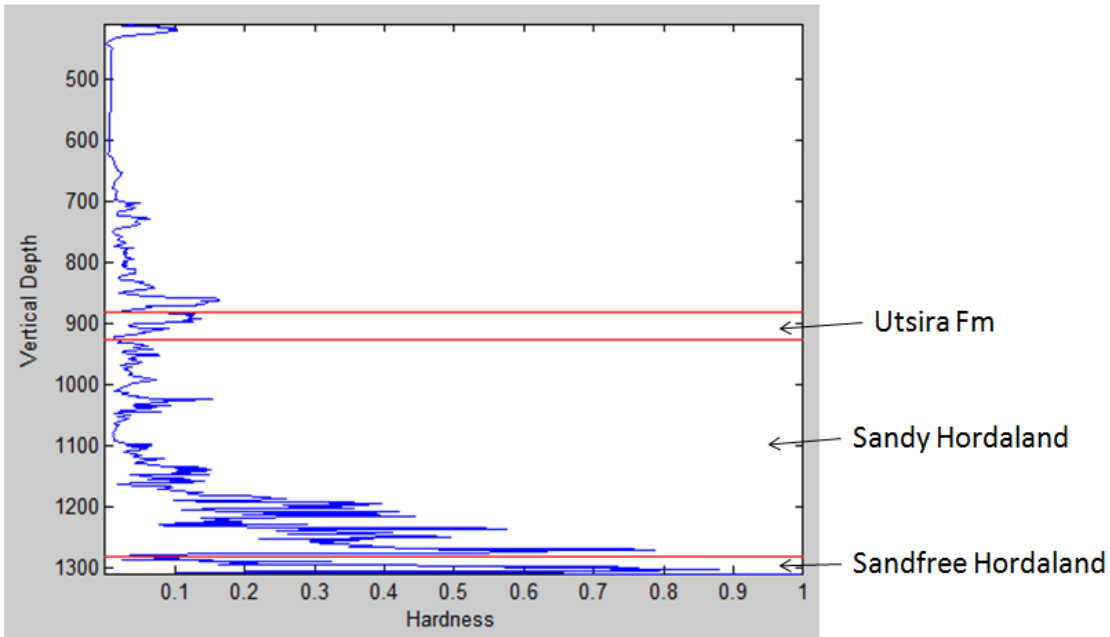
Figure 5-4 Well 0. 24" bit section, interval 436 m to 1 393 m. Hardness is plotted versus vertical depth (m). Utsira Fm. appears between 882 m and 927 m and is located above the sandy Hordaland Fm. Almost no data exist between seabed and 610 m.

As can be seen from Figure 5-4, the hardness is gradually increasing with depth from approximately 610 m and down to 860 m. At approximately 860 m, a harder layer is indicated. This may be an alternative top Utsira Fm due to that the same trend in hardness continues approximately 60 m further down. Figure 5-5 presents a detailed view of Utsira Fm.
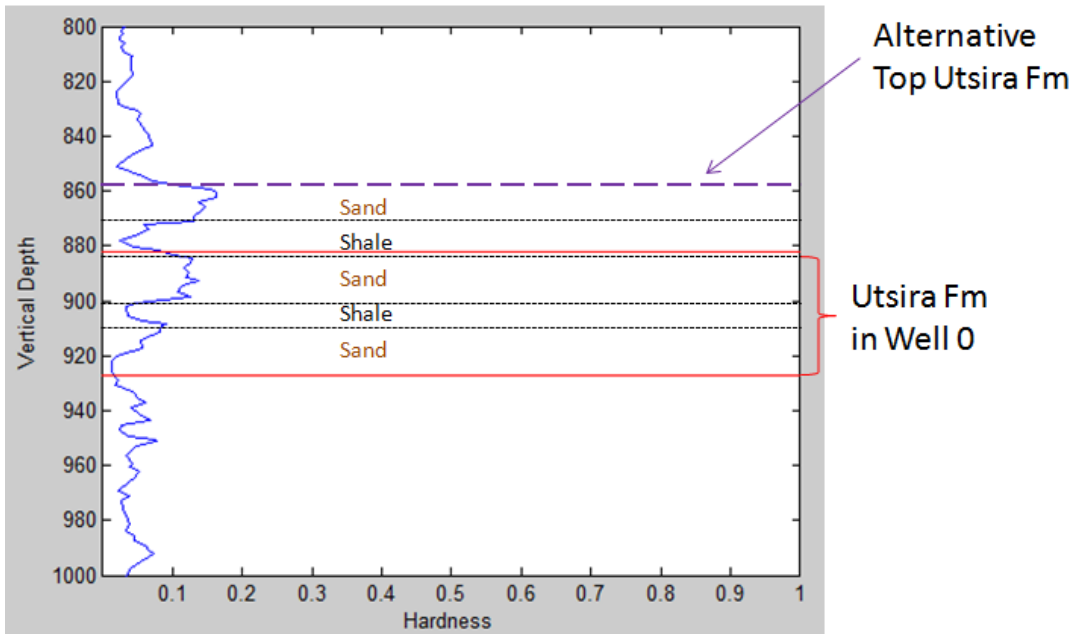
Figure 5-5 Well 0. 24" bit section, interval between 800 m and 1 000 m. Hardness is plotted vs vertical depth (m). The section shows the Utsira Fm and the beginning of Sandy Hordaland Fm. The purple dotted line suggests an alternative upper boundary of the Utsira Fm.

The suggested alternative top Utsira Fm is indicated by a purple stippled line in Figure 5-5. In chapter 5.2 it was assumed that sand is the harder rock type in the formation compared to shale.

Top sandfree Hordaland starts at 1 282 m TVD. Hardness seems to decrease when entering sandfree Hordaland before it starts increasing gradually. The gradual increasing trend is better seen in the 17 ½" section. The 17 ½" bit drills through four different formations. See Figure 5-6.
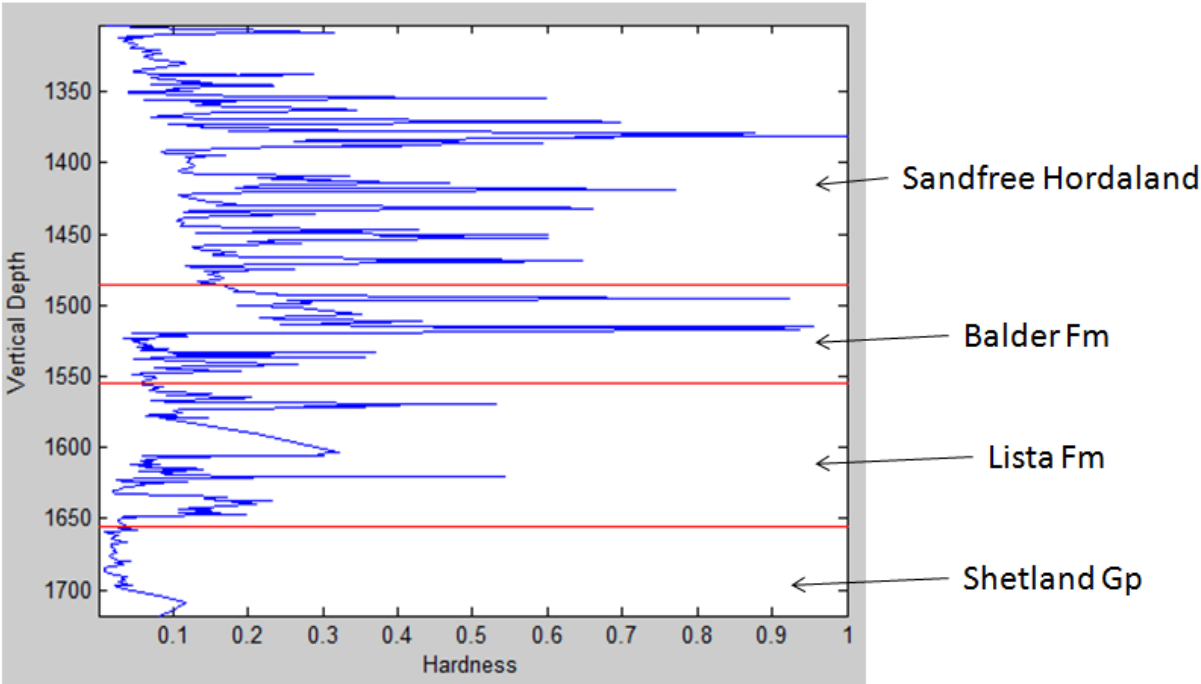
Figure 5-6 Well 0. 17 ½" bit section, interval 1 393m to 1 713 m. Hardness is plotted versus vertical depth (m). The different formations in this section, sandfree Hordaland, Balder Fm, Lista Fm and the Shetland Gp, are illustrated and separated by red lines.

There can be observed some kind of trends of different hardness within the different formations. No magnificent change in hardness may be observed when entering the Balder Fm at the given location. However, there may be indicated a lithology change approximately 30 meters into the given Balder Fm See Figure 5-7.
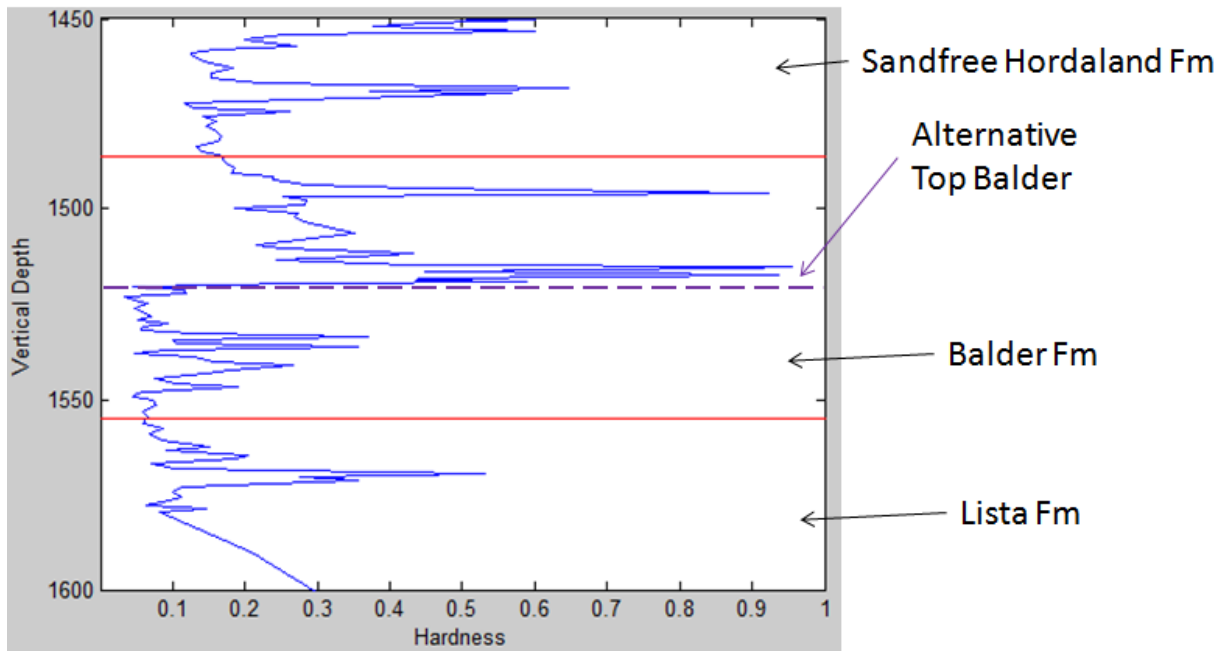
Figure 5-7 Well 0. 17 ½" bit section, interval 1 450 m to 1 600 m. Hardness is plotted versus vertical depth (m). The boundaries of Balder Fm are illustrated by a red line. The purple stippled line indicates an alternative top Balder Fm.

The transition between Lista Fm and Shetland Gp shown in Figure 5-6 is noticeable. This is better seen in Figure 5-8.
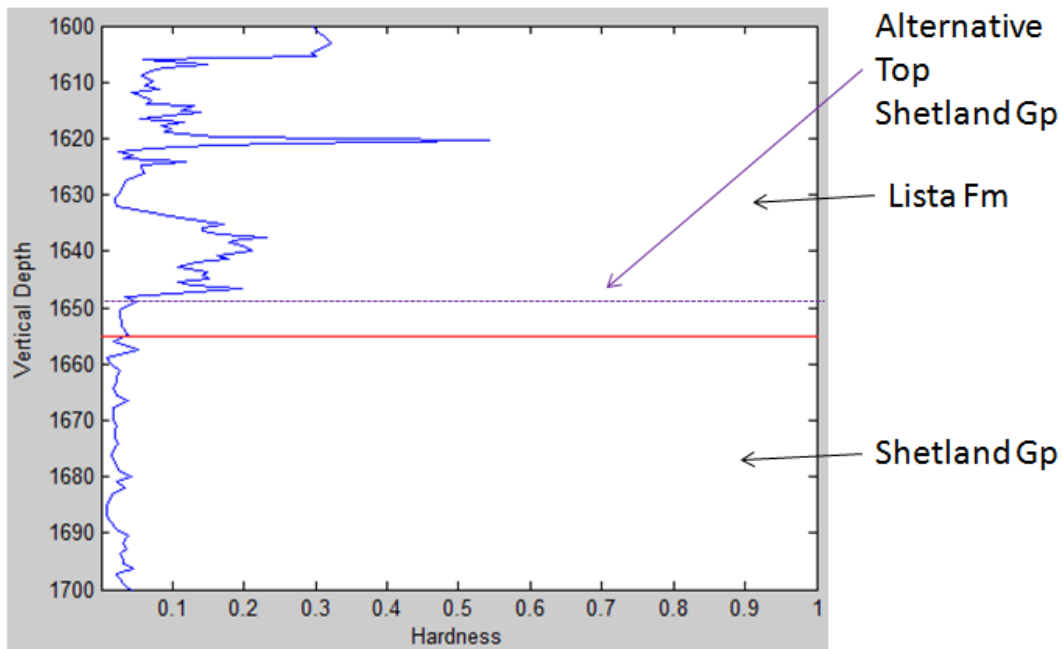
Figure 5-8 Well 0. 17 ½" bit section, interval 1 600 m to 1 700 m. Hardness is plotted versus vertical depth (m). The transition between the Lista Fm and the Shetland Gp is illustrated by a red line. The purple stippled line indicates the appearance of an alternative top Shetland Gp.

The hardness decreases and continues as a quite uniform curve through the Shetland Gp indicating that the calcareous formation is less hard to drill through than the shaly formations positioned above.

6 Analyzing gamma ray and sonic log with respect to hardness and lithology

Gamma ray and acoustic data from Well 0 were not available for present master thesis. However, gamma ray logs and sonic logs were possible to obtain from the Norwegian Petroleum Directory`s (NPD) fact pages for several wells located relatively close to Well 0. These logs have been used for analyses to see if there can be established any possible correlation between hardness and gamma ray and/or sonic log. Figure 6-1 illustrates the distances between Well 0 and the other wells.
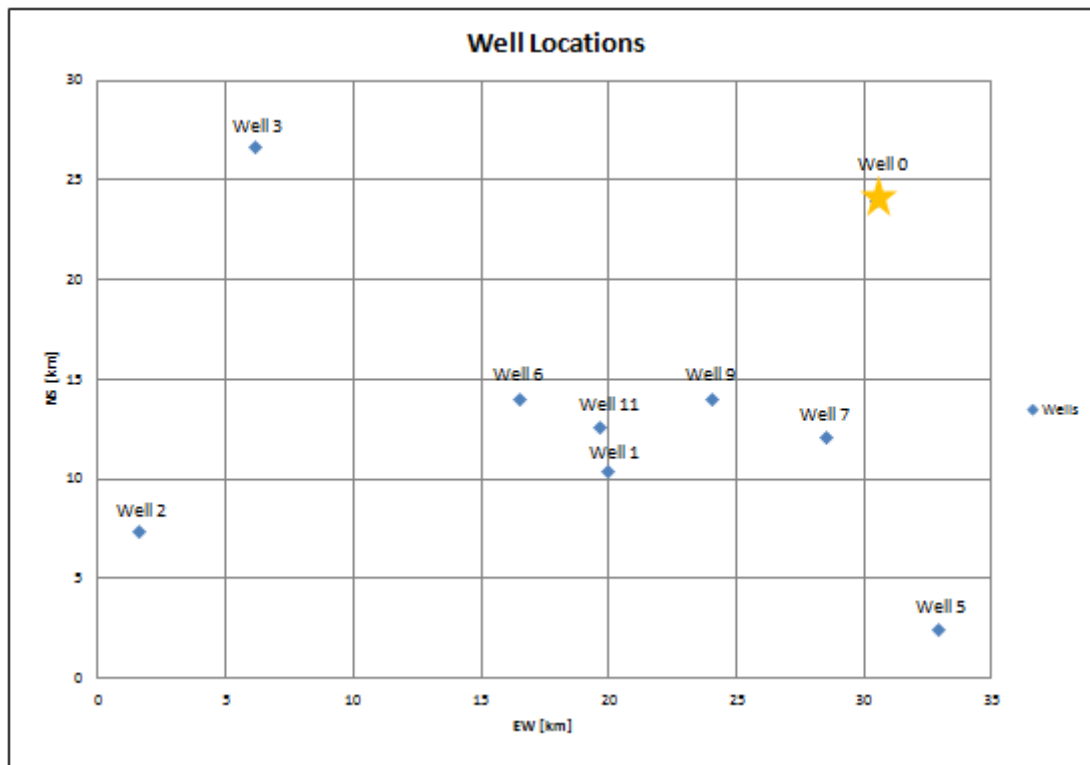
Figure 6-1 Well locations of all wells used in further gamma ray and sonic log analyses in addition to Well 0.

6.1 Gamma Ray vs Hardness/Lithology

The upper boundary of Utsira Fm is normally well defined by a decrease in gamma ray response when leaving the overlying claystones and entering the Utsira Fm (NPD fact pages[6], 2012).

Figure 6-2 illustrates the hardness from Well 0 and the caliper and gamma ray response from the four wells that show the most similar trends.
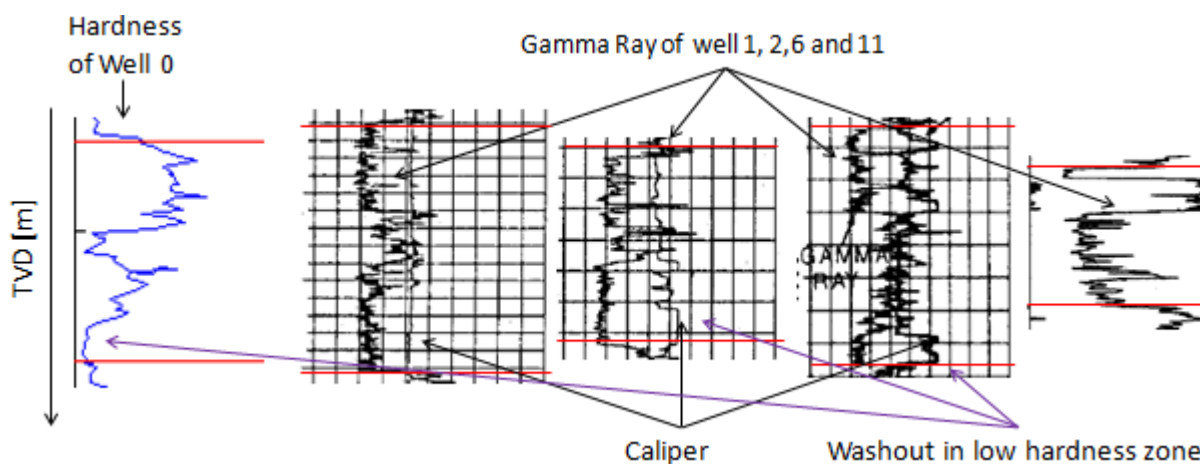
Figure 6-2 Utsira Fm: The hardness curve from Well 0 (left) and the gamma ray and caliper response from the wells 1, 2, 6 and 11 respectively. The red lines indicate the boundary of the Utsira Fm. Utsira Fm is positioned between 882 m and 927 m TVD in Well 0.

The gamma ray readings decrease when entering the Utsira Fm, which is in agreement with the NPD`s characterization of the formation. The gamma ray response also tends to increase when leaving the Utsira Fm (entering the shale again).

The Utsira Formation consists mainly of highly porous and extremely permeable sand which are interbedded by thin layers of shale. As can be seen from Figure 6-2, the Utsira Fm in the wells 1, 2, 6 and 11 consists of three main zones. Two zones contain low gamma ray response, sand, and one zone shows higher gamma ray which is most likely shale or more shaly sand. Sand has been assumed (chapter 5.2) to be harder than shale at this depth. There is a distinct decrease in hardness before leaving the formation which corresponds well with the wells 1, 2, 6 and 11 with respect to entering high level of gamma ray. The gamma ray logs enhance the assumption of sand being harder than shale.

The upper boundary of Balder Fm is defined by the transition from the laminated shales in the formation to the non-laminated, overlying sediments. Normally, this can be seen as an upward reduction in gamma ray response (NPD fact pages[3], 2012).

Figure 6-3 illustrates the gamma ray response in the Balder Fm from four wells in addition to the hardness curve from Well 0.
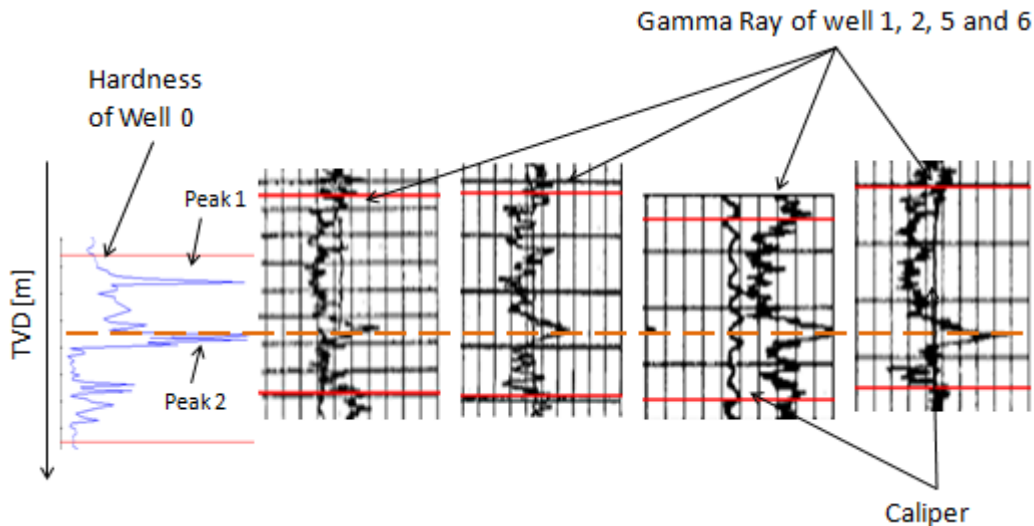
*Figure 6-3 Balder Fm: The hardness curve from Well 0 and the gamma ray and caliper response from the wells 1, 2, 5 and 6 respectively. The red lines illustrate the boundaries of the Balder Fm. A gamma ray and hardness peak is indicated by the yellow dotted line. Balder Fm s positioned between 1 486 m and 1 555 m TVD in Well 0.*

The upward reduction in gamma ray response at the upper boundary of Balder Fm defined by NPD is seen on the logs in Figure 6-3. In addition there is a corresponding increase at the lower boundary. The gamma ray response is quite uniform through the formation in all the wells except from one peak appearing in the middle of the formation. Two peaks are recognized on the hardness curve

Peak 2 is larger than Peak 1 and appears further down in the formation. The hardness peak may result from a hard shale layer and correspond with the common gamma ray peak in the wells illustrated in Figure 6-3. A possible upper hard layer of shale in Balder Fm is seen clearer on the hardness curve than on the gamma ray logs.

The boundary where the Lista Fm and/or Sele Fm are overlain by the Balder Fm is defined by lower gamma-ray readings into the Balder Fm (NPD fact pages[4], 2012). This probably reflects the increase in the tuffaceous components of the Balder Fm (NPD fact pages[3], 2012). In general, the lower boundary of Lista Fm is marked by increased gamma ray readings into a new lithology (NPD fact pages[4], 2012).

Figure 6-4 illustrates the gamma ray response from the Lista Fm. in the five wells where Sele Fm is not present as part of the Rogaland Gr.
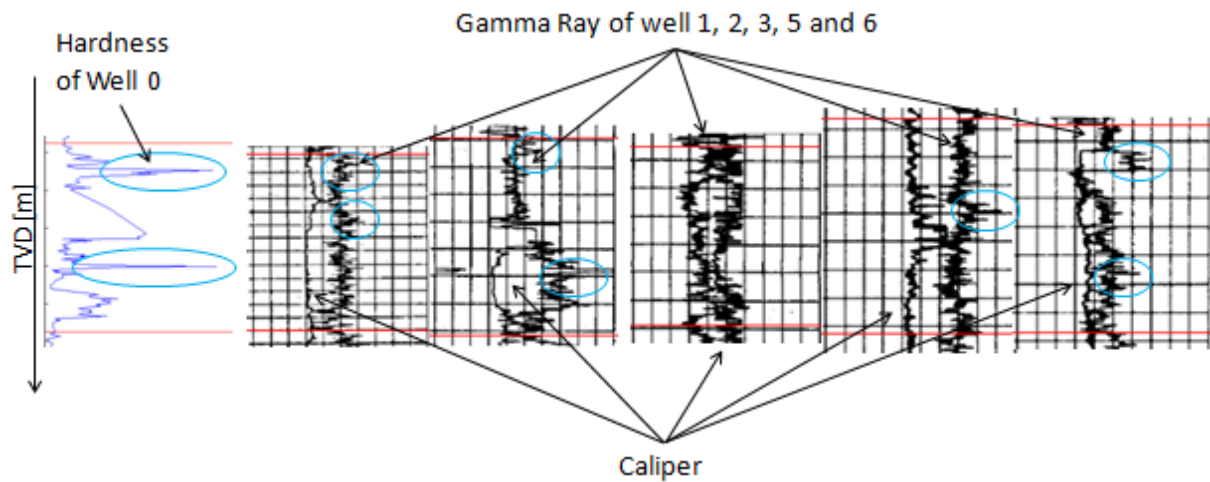
Figure 6-4 Lista Fm: The hardness curve from Well 0 and the gamma ray and caliper response from the wells 1, 2, 3, 5 and 6 respectively. The red lines illustrate the boundaries of the Lista Fm. The blue circles indicate shale and hardness peaks. Lista Fm is positioned between 1 555 m and 1 655 m TVD in Well 0.

NPD`s description of the Lista Fm is clearly seen in well 1, 2, 5 and 6 in Figure 6-4 where the gamma ray response decreases upward at the upper boundary and increases downward at the lower boundary of the formation. The hardness curve shows a slight decrease upward below the upper boundary and may indicate a less hard rock in this area. Due to the uniformity of the gamma ray log, interpretation of this formation is quite hard. However, some shale peaks can be seen on some of the gamma ray logs in Figure 6-4. Two peaks are illustrated on the hardness curve as well.

6.2   Acoustic vs Hardness/Lithology

Acoustic log is commonly used as a synonym for sonic log. It is a display of travel time of acoustic waves versus depth in a well given in time (t) per length (l). The acoustic velocity [t/l] measures the compressional slowness in the formation (Schlumberger[4], 2012). These travel times become faster as the rocks get harder (Spaar, Ledgerwood and Christensen et al., 1995). Figure 6-5 shows the hardness in Well 0 and the sonic response from two other wells with similar behavior in the Utsira Fm.
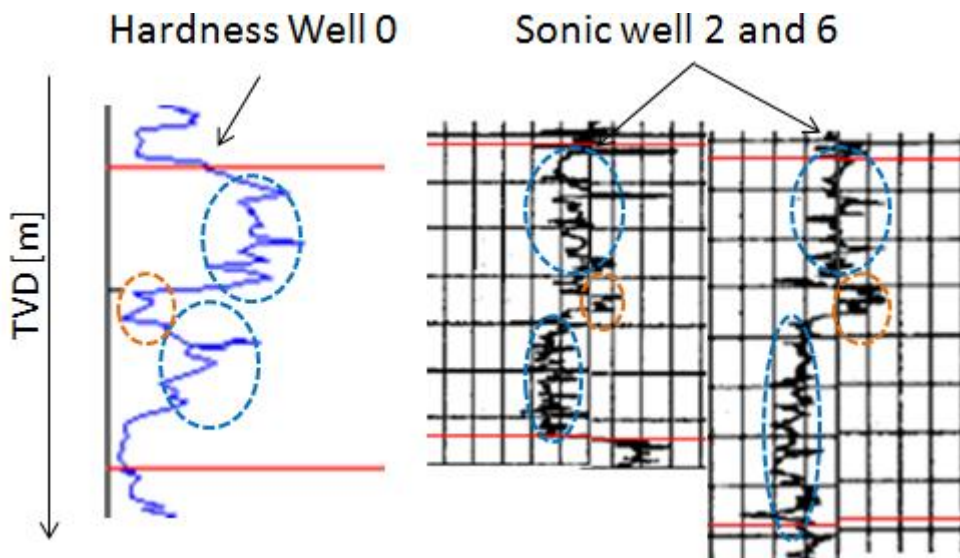
Figure 6-5 Utsira Fm: The hardness in Well 0 and the acoustic response from the wells 2 and 6 respectively. The yellow dotted circles indicate hardness decline and peak on the sonic log, and the blue dotted circles indicate hardness peaks and acoustic declines. Utsira Fm is positioned between 882 m and 927 m TVD in Well 0.

The velocity behavior is fairly similar in well 2 and 6. There is an increase in hardness where the sonic logs increase in the Utsira Fm and vice versa. This is a good fit as the travel time decreases with harder rock.

The upper boundary of the Balder Fm can normally be seen as an upward reduction in sonic log (NPD fact pages[3], 2012). The lower boundary of the Balder Fm, the transition into the Lista Fm, is defined by a downward reduction in sonic velocity (NPD fact pages[4], 2012).

Figure 6-6 shows the hardness in Well 0 and the acoustic response from two wells recorded from the Balder Fm.
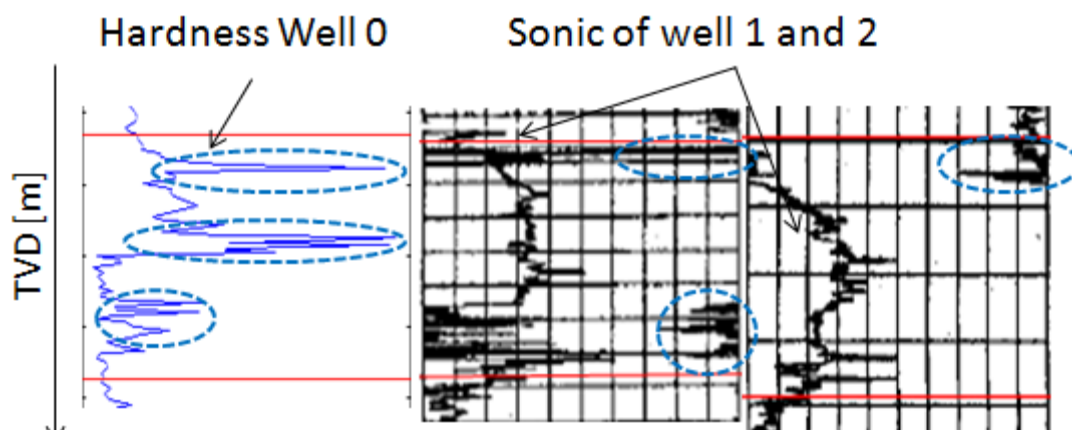
Figure 6-6 Balder Fm: The hardness in Well 0 and the acoustic response from the wells 1 and 2 respectively. The lower and upper boundaries of the formation are illustrated by a red line. The blue dotted circles indicate shale peaks. Balder Fm is positioned between 1 555 m TVD in Well 0.

Both statements mentioned above regarding sonic velocity change due to entering and leaving the Balder Fm can be seen in Figure 6-6. The velocity increases into the formation and decreases on its way out. Some of the three peaks observed on the hardness curve are recognized on the sonic log in well 1 and 2. However, the peak appearing in the middle of the formation in Well 0 is not recognized on any sonic log analyzed in present work.

Figure 6-7 shows the hardness in Well 0 and the acoustic response from two wells recorded in the Lista Fm.
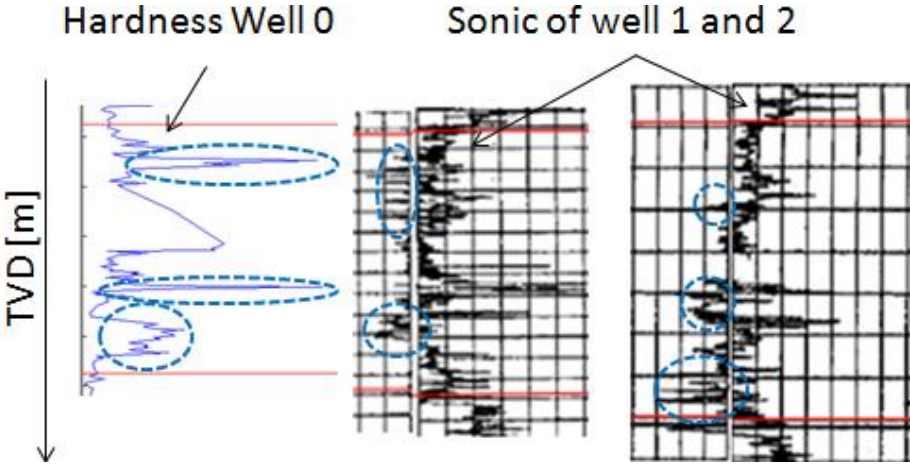
Figure 6-7 Lista Fm: The hardness in Well 0 and the acoustic response from the wells 1 and 2 respectively. The lower and upper boundaries of the formation are illustrated by a red line. The blue dotted circles indicate shale peaks. Lista Fm is positioned between 1 555 m and 1 655 m TVD in Well 0.

The velocity is fairly uniform through the Lista Fm. However, some peaks seen on the hardness curve are recognized as declines on the sonic log in well 1 and 2 indicating shale.

Figure 6-8 is an illustration of hardness and the assumed gamma ray and sonic log from Well 0 based on the logs from wells nearby. Types of formations are indicated based on analyses from chapter 5.2 where sand is indicates harder than shale above approximately 1 500 m.
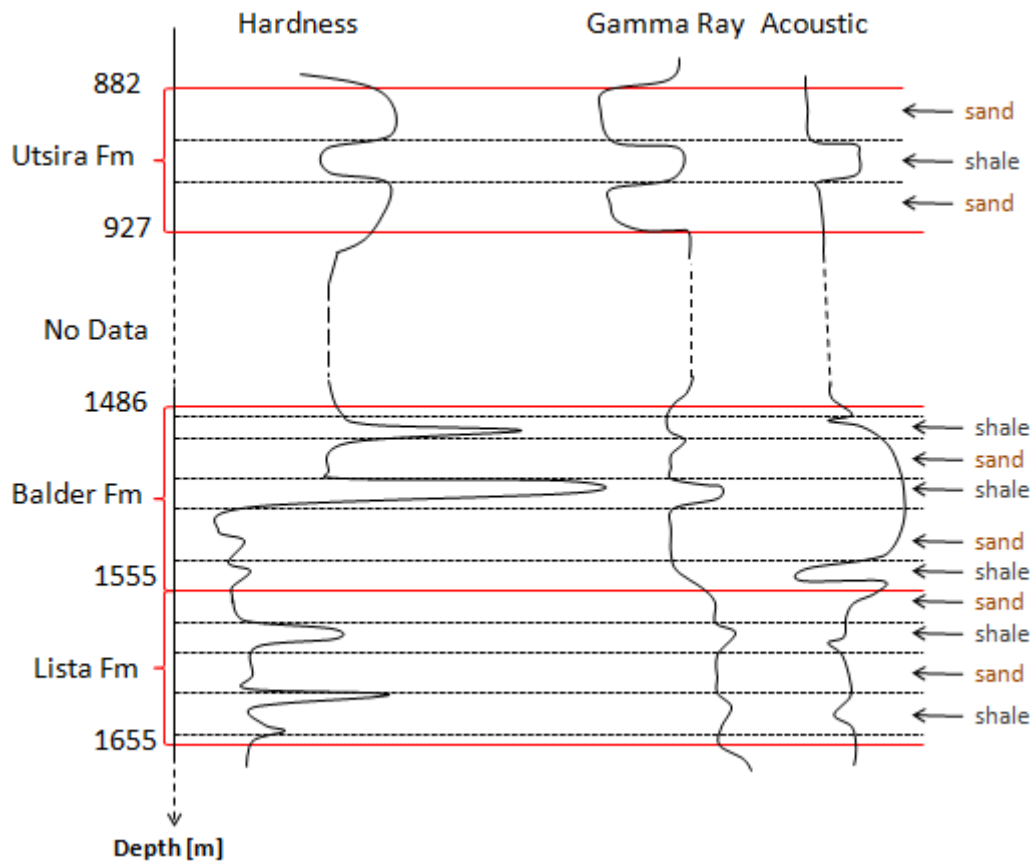
Figure 6-8 Well 0. Hardness and the gamma ray (assumed on bases of neighboring data) and sonic (assumed on bases of neighboring data) logs are drawn. Sands are assumed to be harder than shale at depths above approximately 1 500 m and shale are harder than sand at depths below.

7 Discussion

Hard stringers have been indicated in Well 0 by calculating drillability (the inverse of hardness) through a simplified version of the ROP equation (4-4) proposed by Bourgoyne and Young (1986). Real-time drilling data have been utilized as input parameters in the equation. Due to the complexity of the drillability computation, simplifications had to be made to obtain the result presented in present master thesis. The impact these simplifications have on the final result is discussed below. The correlations established between hardness and lithology and hardness and both sonic and gamma ray have also been evaluated.

7.1 Quality of Mathematical Model

The quality is mainly related to the model, which could be improved to fit the physics of the real world, i.e. less simplifying assumptions (Solberg, 2011):

The exponents related to WOB and RPM and the threshold bit weight will frequently vary with the hardness of the formation. The difference in hardness between hard and soft formations is shown to be more distinct when applying exponents related to harder formations. This was illustrated in Figure 4-13. However, the transitions between soft and hard formations are evidently seen in both cases. One way to achieve more accurate hardness values is to constantly vary the fitted exponents to the formations drilled. This may be obtained by first calculating hardness in the whole well by using only one exponent for both WOB and RPM. Then normalize the hardness to range from 0 to 1 by dividing all hardness values by the largest hardness in the section. Then use the hardness scale to classify the formations with respect to hardness. During present thesis the formations were classified in two categories;

1. Soft formations: hardness < 0.5
2. Hard formations: hardness > 0.5

This approach will most likely be improved by adding more categories, e.g extremely hard, very hard, medium hard, medium soft, very soft etc. However, the difference is not assumed significant enough to affect the detection of hard stringers required in present work. Reducing the drillability definition in hard formations from less than 0.5 to less than 0.3 has impact on the hardness curve (See Figure 4-14). However, changing the drillability classification did not have any effect upon the sudden change in hardness. The threshold bit weight is minimal in soft formations and hard to evaluate. The affect of threshold bit weight on the final result is assumed negligible.

The function related to change in depth given by equation 3-2 models the effect of compaction on the penetration rate and accounts for increased strength due to normal compaction with depth (Solberg, 2011). The depth correction exponent was determined during present master thesis through linear regression (see results chapter 3.2.2). The determined factor made hardness uniformly decrease with depth which most likely is due to too large depth correction exponent (See Figure 4-19 and 4-21). However, decreasing the exponent by a tenth resulted in a negligible correction factor (See Figure 4-20 and 4-22). The exact value of hardness is of no interest in present thesis and the factor was proved not to affect the sudden change in hardness.

The changes of penetration rate due to tooth wear, under-compaction and variety due to mud weight have not been utilized in the determination of drillability (hardness). One common reason for all the factors is that they make rather complex functions through real-time drilling data (Solberg, 2011). The factors` impact on ROP is further discussed below.

It is common that the drill bit tends to wear as the bit run progresses. The wear of the drill bit may result in a less effective penetration. When comparing hardness in a shallow section with hardness calculated in a deeper formation, the bit tooth wear should be considered. However, the wear process appears gradually and will not affect the sudden change in hardness.

The under-compaction function models the effect of under-compaction appearing in abnormally pressured formations. Under-compaction is of importance for the final result as an under-compacted layer will act as a soft formation. However, hardness detection is mainly about distinguishing between hard and soft formations. Under-compaction may only be relevant when determining the lithology of the formation.

Mud weight`s affect on hardness detection has been neglected. However, mud weight should be considered when using ROP to estimate hardness. This is further discussed during "Future Improvemnets".

Sand has been asumed harder than shale in shallow formations due to diagenesis of shale discussed in chapter 5.2. This assumption was enhanced when comparing hardness and gamma ray responses from Utsira Fm (882 m - 927 m). Gamma ray peaks in Balder Fm and Lista Fm were recognized on the hardness plot and could indicate hard stringers due to shale being harder than sand at these depths.

Correlation can be established between hardness and acoustic response from the logs analyzed during present master thesis. Especially hardness in the Utsira Fm showed evident correlation with the sonic logs from at least two wells (See Figure 6-5). Increase in hardness correlates with reduction in acoustic and vice versa. Some peaks observed on the hardness curve could be recognized as declines on some sonic logs originating from the Balder and Lista formations. However, not all the wells showed good correlations with the hardness curve, and due to absence of gamma ray and acoustic data in Well 0 it is difficult to determine the accuracy of the correlations established.

Lithology changes are recognizable on the hardness curve. In the middle of Balder Fm the lithology alters from quite hard to softer layers. The transition from the Lista Fm into the softer calcareous Shetland Gp is evident. However, other indicators like sonic and gamma ray logs are necessary to establish the accuracy of the indications made by the hardness curve.

7.2 Quality of Data

Most of the test data employed in present master thesis are of good quality. RPM and WOB recorded from Well 0 are proved to correspond well with the velocity of BPOS. However, some unlikely low values of RPM and WOB were experienced. Low RPM and WOB data were most likely recorded during other operations than drilling and have therefore been excluded in the calculations of drillability (Solberg, 2011).

The rate of penetration data given together with the real-time drilling data have been estimated by the data service company. The given rate of penetration should be equal to the velocity of the block. However, comparison of ROP and ΔBPOS (Figure 4-4) shows that they only correspond to some degree. They show the same trend, but the service company`s estimated ROP appears deeper than the calculated ΔBPOS. It is unknown how the service company has made their estimation of ROP. Using the estimated ROP instead of ΔBPOS will make the indicated hard stringers appear deeper than where they are actually located.

ΔBPOS has been estimated by using simple calculations. After computing the average of three or more block positions, the slope between two average block positions were determined. This determination of ΔBPOS may result in some inaccurate values of block velocity. However, the exact value of hardness is of no interest in present thesis. The calculated block velocities are accurate enough to distinguish between relatively hard and relatively soft stringers.

Sonic and gamma ray log from Well 0 were not available. The calculated hardness had to be compared with sonic and gamma ray logs from different wells located in the same area. Since the correlation between hardness and the two log types, especially the sonic log, is defected, the trustworthiness of the correlation is hard to evaluate. Logs from some of the wells did not show any particular correlation with the hardness log. Such relations are difficult to establish if no quality data from the same well is obtainable.

7.3 Future Improvements

Present master thesis is a preliminary work for further investigation of drillability and its relation to soft and hard stringers. Automatic detection of hard and soft formations through real-time drilling data is proved to be an effective way to determine the formation hardness. The detection tool is both cost-effective and practical since transitions between hard and soft stringers contribute to severe downhole problems. However, there are many potential improvements to present work;

1. The accuracy of the predictions made during present master thesis is hard to evaluate. Testing the program with data from several different wells is necessary in order to establish better correlation between real hardness and hardness indicated by the program.

2. A future version should contain fewer simplifications. All simplifications made during present work contribute to a degree of error in the calculations of drillability.

3. All the functional relations from the Bourgoyne and Young equation are functions of formation types and can be verified by previous drilling experiences in the field. Each functional relation has an empirical exponent or constant that relates to them. The exponents of RPM and WOB were proved to affect the value of drillability and should be adjusted continuously as the drillability and hardness change with the formation. Altering all the exponents or constants correctly is difficult to achieve and is definitely a challenging task.

4. The pore pressure in the formation generally increases with depth. To maintain the stability of the hole the mud weight is then increased which may lead to increased ΔP (the difference between the hydrostatic pressure column (MW) in the well and the pore pressure). Increasing ΔP will lead to a decreasing rate of penetration. Decrease in ROP due to increase in MW may appear as a hard formation on the hardness plot. Considering mud weight`s impact on ROP when calculating hardness should definitely be part of future work.

5. Correlating gamma ray and acoustic data with calculated hardness using data recorded from the same well is a prerequisite for future work. It would help evaluating the quality of present work, especially as sonic log is a great indicator of hard formations.

6. Together with the ROP equation by Bourgoyne and Young (1986) the normalized ROP equation (2-3) proposed by Provost (1987) was presented in chapter 2. The normalized ROP indicates what the drilling rate should be if all other parameters are held constant. The plot was claimed effective for lithology prediction and shows significantly slower drilling rate in sand-shales than in sand zones at the same depth. Unfortunately, most parameters in the normalized ROP equation are not obtainable directly through real-time drilling data. Suggestion for future work is to test the normalized ROP model together with the model analyzed during present work to look for lithology correlations.

8   Conclusion

On basis of the work done in present master thesis, following statements can be made;

Several different problems are related to hard stringers and hard stringers are therefore important to detect. Much theoretical work has been done to make the most accurate approach concerning drillability (hardness) in order to detect hard stringers.

The Model:

- The calculations of drillability are based on a simplified version of the ROP equation proposed by Bourgoyne and Young (1986). The simplified model results in some degree of error to the drillability calculations.

- An improved and modified Matlab program previously created by Solberg (2011) has been applied in the calculations of drillability. WOB, RPM and BPOS obtained from real-time drilling data have been utilized as input parameters in the equation. The final result shows a plot of hardness variation with depth.

- The WOB and RPM exponents have been classified in two categories. Using different exponent values were proved to affect the hardness plot, but not to affect the detection of hard stringers. Changing the classification of hard formations from drillability less than 0.5 to drillability less than 0.3 were proved to not affect the sudden change in hardness. The depth correction factor was proved not to affect hardness detection.

The Data:

- The ROP given in real-time drilling data is estimated by the service company and proved to be of not so good quality. Penetration rates applied in present work was therefore calculated using the movement of the block. The estimated ROP and the calculated block velocity show the same trend and to some degree the same values, but the estimated ROP do not correspond with the same measured depth as the block velocity.

Results and Analyses:

- Hard stringers were indicated by the hardness plot. The indications of hard stringers were enhanced by manual analyses together with experienced hard stringers expressed in the Final Well Report.

- Lithology transitions have been indicated by the hardness plot.

- Correlations between the hardness plot and gamma ray logs and the hardness plot and sonic logs from wells nearby have been established.

9 References

About.com a – Part of The New York Times Company. Shale, http://geology.about.com/od/rocks/ig/sedrockindex/rocpicshale.htm. Cited 25 April 2012

About.com b – Part of The New York Times Company. Slate, http://geology.about.com/od/rocks/ig/metrockindex/rocpicslate.htm. Cited 25 April 2012

About.com c – Part of The New York Times Company. Muscovite Mica, http://geology.about.com/od/minerals/ig/minpicrockforming/minpicmuscovite.htm. Cited 25 April 2012

Albertin, M.L., Petmecky, S. and Jay, C., et al. 2003. Drillability Assessment in Deepwater Exploration. Paper OTC 15295 presented at the Offshore Technology Conference, Houston, Texas, , 5-8 May. DOI: 10.4043/15295-MS

Alum, M.A., Egbon, F. 2011. Semi-Analytical Models on the Effect of Drilling Fluid Properties on Rate of Penetration (ROP). Paper SPE 150806 presented at the Nigeria Annual International Conference and Exhibition, Abuja, Nigeria, 30 July - 3 August. DOI: 10.2118/150806-MS

Andrews,R., Nygaard, G., and Engler, R. et al. 2007. Methods of Using Logs to Quantify Drillability. Paper SPE 106571 presented at the 2007 SPE Rocky Mountain Oil & Gas Technology Symposium, Denver, USA, 16 - 18 April. DOI: 10.2118/106571-MS

Aron, J.,Chang, S.K., Codazzi, D. et al. 1997. Real-Time Sonic Logging While Drilling in Hard and Soft Rocks. Paper SPWLA 1997-HH presented at the 38th Annual Logging Symposium, Sugar Land, Texas, 15-18 June

Bahari, M.H., Bahari,A., and Moharrami,F.N. et al. 2008. Determining Bourgoyne and Young Model Coefficients Using Genetic Algorithm to Predict Drilling Rate. Journal of Applied Sciences **8**: 3050-3054. DOI: 10.3923/jas.2008.3050.3054. Available at http://scialert.net/fulltext/?doi=jas.2008.3050.3054. Cited 09.03.12. 8: 3050-3054.

Bahari, A., Baradaran, A. 2007. Trust-Region Approach To Find Constants of Bourgoyne and Young Penetration Rate Model in Khangiran Iranian Gas Field. Paper SPE 107520 presented at the SPE Latin American and Carribean Petroleum Engineering Conference, Buenos Aires, 15-18 April. DOI: 10.2118/107520-MS

Bielstein, W.J, Cannon, G.E. 1950. Factors Affecting the Rate of Penetration of Rock Bits. Paper API 50-061 presented at the spring meeting, South-western District, Division of Production, Dallas, USA, March

Bourgoyne, A.T., Millhelm, K.K., and Chenevert, M.E. et al. 1986. Applied drilling Engineering. Textbook Series, SPE, Richardson, Texas **2**: 221-235

Bourgoyne, A.T.,Young., F.S. 1973. The Use of Drillability Logs for Formation Evaluation and Abnormal Pressure Detection. Paper SPWLA 1973-T presented at the fourteenth annual logging symposium, 6-9 may

Bourgoyne, A.T.,Young, F.S. 1974. A Multiple Regression Approach to Optimal Drilling and Abnormal Pressure Detection. *J. SPE* **14**(4): 371-384. SPE 4238-PA. DOI: 10.2118/4238-PA.

Cheniany, A., Khoshrou, S.H., Shahriar,K. et al. 2010. Estimation of Penetration Rate of Rotary Drills using a New Drillability Index in Sarcheshmeh Copper Mine. Paper ISRM ARMS6-2010-153 presented at the ISRM International Symposium 2010 and 6th Asian Rock Mechanics Symposium – Advances in Rock Engineering, New Delhi, India, 23-27 October

Cunningham, R.A., Goins, W.C. 1960. Laboratory Studies of the Effect of Rotary Speed on Rock-bit Performance and Drilling Cost. Paper API 60-007 presented at the spring meeting of the Mid-Continent District, Division of Production, Wichita, Kans, 30 March- 1 April.

Dvornikov, L.T. 1964. Investigation of some questions concerning rotary drilling of boreholes in rocks of medium hardness, Tomsk, Russia

Eslinger, E. and Peaver, D., 1988. Clay minerals for petroleum geologists and engineers. Chap. 5: Shale diagenesis. SEPM Short course, Tulsa **22:** 5-1 - 5-42.

Christophersen, L., Gjerde, J., Valdem, S. 2007. Final Well Report. Statoil, Bergen

Garnier, A.J., Van Ingen, N.H. Phenomena Affecting Drilling Rates at Depth. 1958. Trans., AIME **216:** 232-239

Gstalder, S., Raynal, J. 1966. Measurement of Some Mechanical Properties of Rocks and Their Relationship to Rock Drillability. *J. Pet Tech* **18** (8): 991-996. SPE-1463-PA. DOI: 10.2118/1463-PA

Head, A.L. 1951. A Drillability Classification of Geological Formations. Paper WPC 4105 presented at the 3rd World Petroleum Congress, Hague, Netherland, 28 May – 6 June

Hongjin, Y. 1986. Investigation on the Application of Statistical Formation Drillability. Paper SPE 14848 presented at the International Meeting on Petroleum Engineering, Beijing, China, 17-20 March. DOI: 10.2118/14848-MS

Hood,J,Hovden,J,Heisig,G et al. 2003. Real-Time BHA Bending Information Reduces Risk when Drilling Hard Interbedded Formations. Paper SPE 79918 presented at the SPE/IADC Drilling Conference, Amsterdam, Netherland, 19-21 February. DOI: 10.2118/79918-MS

Koederitz, W.L., Johnson, W.E. 2011. Real-Time Optimization of Drilling Parameters by Autonomous, Empirical Methods. Paper SPE 139849 presented at the SPE/IADC Drilling Conference and Exhibition held in Amsterdam, Netherlands, 1-3 March. DOI: 10.2118/139849-MS

Langeland, H. 1992. Innføring i Boreholslogging. Trondheim. Langeland, 175-205

Markman, L.D. 1971. Formula for Rotary Drilling. Journal of Science Mining **7**(5): 542. DOI: 10.1007/BF02501066

NPD fact pages[1]. Hordaland Group, http://www.npd.no/engelsk/cwi/pbl/en/su/all/67.htm. Cited 5 March 2012

NPD fact pages[2]. Rogaland Group, http://www.npd.no/engelsk/cwi/pbl/en/su/all/131.htm. Cited 24 April 2012

NPD fact pages[3]. Balder Formation, http://www.npd.no/engelsk/cwi/pbl/en/su/all/6.htm. Cited 2 February 2012

NPD fact pages[4]. Lista Formation, http://www.npd.no/engelsk/cwi/pbl/en/su/all/95.htm. Cited 2 February 2012

NPD fact pages[5]. Shetland Group, http://www.npd.no/engelsk/cwi/pbl/en/su/all/143.htm. Cited 2 February 2012

NPD fact pages[6]. Utsira Formation, http://www.npd.no/engelsk/cwi/pbl/en/su/all/183.htm. Cited 20 March 2012

Onyia, E.C. 1988. Relationship Between Formation Strength, Drilling Strength and Electric Log Properties. Paper SPE 18166 prepared for presentation at the 63rd Annual Technical Conference and Exhibition of the Society of Petroleum Engineers held in Houston, Texas, 2-5 October. DOI: 10.2118/18166-MS

Overton, H.L., 1973. A Dimensionally Derived Rock Drillability Equation. Paper SPE 4237 presented at the Sixth Conference on Drilling and Rock Mechanics, Austin, Texas, 22-23 January. DOI: 10.2118/4237-MS

Pore Pressure. Under-compaction. Available at http://www.porepressure.info/Undercompaction.html. Cited 26 January 2012

Prasad, U. 2009. Drillability of a Rock in Terms of its Physico-Mechanical and Micro-Structural Properties. Paper ARMA 09-040 presented at Asheville 2009, the 43rd US Rock Mechanics Symposium and 4th U.S.-Canada Rock Mechanics Symposium, Asheville, North Carolina, 28 June - 1 July

Prestvik, T. 2001. Petrologi og Geokjemi. Trondheim, Vett & Viten AS, 125-131

Provost, C.E. 1987. A Real-Time Normalized Rate of Penetration Aids in Lithology and Pore Pressure Prediction. Paper SPE 16165 presented at the SPE/IADC Drilling Conference, New Orleans, Louisiana, 15-18 March. DOI: 10.2118/16165-MS

Rashidi, B., Hareland, G., Shirkavand, F. 2009. Lithological determination from logs. Paper PETSOC 2009-180 presented at the Canadian International Petroleum Conference, Calgary, Alberta, 16-18 June. DOI 10.2118/2009-180

Saif, M.A.A. 1982. Can We Increase Both Penetration Rate and Bit Footage in Hard and Very Hard Formations. Paper SPE 10887 presented at the Rocky Mountain Regional Meeting of the Society of Petroleum Engineers, Billings, Montana, 19-21 May. DOI: 10.2118/10887-MS

Schlumberger[1]. Washouts, Available at http://www.glossary.oilfield.slb.com/search.cfm. Cited 07 March 2011

Schlumberger[2]. Dogleg, http://www.glossary.oilfield.slb.com/search.cfm. Cited 07 March 2011

Schlumberger[3]. Keyseat, http://www.glossary.oilfield.slb.com/search.cfm. Cited 07 March 2011

Schlumberger[4]. Acoustic Log, http://www.glossary.oilfield.slb.com/Display.cfm?Term=acoustic%20log. Cited 20 March 2012

Solberg, S.M. 2011. Detection of Hard Stringers from Real-Time Drilling Data. Project, NTNU, Trondheim, Norway.

Somerton, W.H., Esfandiari, F., Simghal, A. 1969. Further Studies of the Relation of Physical Properties of Rock to Rock Drillability. Paper SPE 2390 presented at the Drilling and Rock Mechanics Symposium, Austin, Texas, 14-15 January.DOI: 10.2118/2390-MS

Somerton, W.H. A Laboratory Study of Rock Breakage by Rotary Drilling. 1959. Trans., AIME **216**: 92-97.

Spaar, J.R., Ledgerwood, L.W., Christensen, H. et al. 1995. Formation Compressive Strength Estimates for Predicting Drillability and PDC Bit Selection. Paper SPE 29397 presented at the SPE/IADC Drilling Conference, Amsterdam, Netherland, 28 February- 2March. DOI: 10.2118/29397-MS

Talabani, S., Chukwu, G., Hatzignatiou, D. 1993. Drilling Successfully Through Shale Formations: Case Histories. Paper SPE 25867 presented at the Rocky Mountain Regional/Low Permeability Reservoirs Symposium, Denver, Colorado, 12 -14 April. DOI: 10.2118/25867-MS

The Free Dictionary. Formation, http://www.thefreedictionary.com/formation. Cited 5 March 2012

Wu, A., Hareland, G., Rashidi, B. 2010. The Effect of Different Rock Types and Roller Cone Insert Types and Wear on ROP (Rate of Penetration). Paper ARMA 10-207 presented at the 44th US Rock Mechanics Symposium and 5th US-Canada Rock Mechanics Symposium, Salt Lake City, Utah, 27-30 June

Young, F.S. 1969. Computerized Drilling Control. *J. Pet Tech* **21**(4): 483-496. SPE 2241-PA. DOI: 10.2118/2241-PA

Young, J.H. 1980. Spectral Gamma-Ray (KUT) Borehole Logging. Paper SPE 9465 presented at the 55th annual fall technical conference and exhibition of the society of petroleum engineers of AIME, Dallas, Texas, 21-24 September. DOI: 10.2118/9465-MS

Zweigel,P ,Arts,R, Lothe,A.E. et al. 2004. Reservoir geology of the Utsira Formation at the first industrial-scale underground CO_2 storage site (Sleipner area, NorthSea). The Geological Society **233**: 165-180.

10 Abbreviations

BHA	Bore Hole Assembly
BPOS	Block Position
DBTM	Bit Measured Depth
DMEA	Measured Depth
DVER	Vertical Depth
FWR	Final Well Report
GR	Gamma Ray
HLD	High Local Dogleg
HLD	High Local Dogleg
MD	Measured Depth
NROP	Normalized Rate Of Penetration
ROP	Rate Of Penetration
RPM	Rotary Speed
TVD	True Vertical Depth
WOB	Weight On Bit
ΔBPOS	Block Position Velocity
ΔP	Pressure Difference

11 Appendix

The Matlab program consists of one main program and several executing functions.

11.1 The main program

```matlab
clc
clear

%put filenames into a list
    filename{1} = 'LT122205.ASC.h5';
    filename{2} = 'LT122305.ASC.h5';
    filename{3} = 'LT122405.ASC.h5';
    filename{4} = 'LT122505.ASC.h5';
    filename{5} = 'LT010106.ASC.h5';
    filename{6} = 'LT010206.ASC.h5';
    filename{7} = 'LT010406.ASC.h5';
    filename{8} = 'LT010506.ASC.h5';

%count number of files
NrOfFiles = length(filename);

a = '/WOB';
b = '/RPMB';
c = '/DBTM';
d = '/DMEA';
e = '/Time';
f = '/BPOS';
g = '/ROP';
h = '/DVER';

%inputs:
a2 = 0.0001;
a5_ave = 1.2;
a6_ave = 0.6;

a5_soft = 2.0;
a6_soft = 0.9;

a5_hard = 0.6;
a6_hard = 0.4;

j=1;
for i = 1:1:NrOfFiles
    WOB = 0;
    RPM = 0;
    DBTM = 0;
    DMEA = 0;
    time = 0;
    BPOS = 0;
    ROP = 0;
    DVER = 0;
    WOB = h5read(filename{i},a);
    RPM = h5read(filename{i},b);
    DMEA = h5read(filename{i},c);
    DBTM = h5read(filename{i},d);
    time = h5read(filename{i},e);
    BPOS = h5read(filename{i},f);
    ROP = h5read(filename{i},g);
    DVER = h5read(filename{i},h);

    %check what operation this file contains
    if min(DMEA) == max(DMEA)

    disp(['No drilling in this section. Measured depth is: ' num2str(DMEA(list))]);
```

```matlab
        else

        disp('operation: drilling')
        disp(['start drilling at: ', num2str(min(DMEA))]);
        disp(['stop drilling at: ', num2str(max(DMEA))]);

        list = length(WOB);

            for k =1:1:list

                WOB_list(j+k-1) = WOB(k);
                RPM_list(j+k-1) = RPM(k);
                DBTM_list(j+k-1) = DBTM(k);
                DMEA_list(j+k-1) = DMEA(k);
                time_list(j+k-1) = time(k);
                BPOS_list(j+k-1) = BPOS(k);
                ROP_list(j+k-1) = ROP(k);
                DVER_list(j+k-1) = DVER(k);

            end

    end
            j = j + k;
end

list = length(WOB_list);

%Eliminate odd values of WOB and RPM
[list WOB_el RPM_el DBTM_el DMEA_el time_el BPOS_el, ROP_el, DVER_el] =
eliminate_WOB(list, WOB_list, RPM_list, DBTM_list, DMEA_list,...
time_list, BPOS_list, ROP_list, DVER_list);

[list WOB_el2 RPM_el2 DBTM_el2 DMEA_el2 time_el2 BPOS_el2, ROP_el2, DVER_el2] =
eliminate_RPM(list, WOB_el, RPM_el, DBTM_el, DMEA_el,...
time_el, BPOS_el, ROP_el, DVER_el);

[list WOB_el3 RPM_el3 DBTM_el3 DMEA_el3 time_el3 BPOS_el3, ROP_el3, DVER_el3] =
eliminate_DMEA(list, WOB_el2, RPM_el2, DBTM_el2, DMEA_el2,...
time_el2, BPOS_el2, ROP_el2, DVER_el2);

%sort lists of data with regard to measured depth
[matrix_sorted] = sort_rows(list, WOB_el3, RPM_el3, DBTM_el3, DMEA_el3, time_el3,
BPOS_el3, ROP_el3, DVER_el3);

%compute average of all data
[list matrix_ave] = compute_average(list, matrix_sorted);

%compute dBPOS
[listo WOB_db RPM_db DBTM_db DMEA_db time_db BPOS_db ROP_db DVER_db dBPOS_db] =
Compute_dBPOS(list, matrix_ave);

%eliminate odd values of dBPOS
[list WOB_cor RPM_cor DBTM_cor DMEA_cor time_cor BPOS_cor ROP_cor DVER_cor
dBPOS_cor] = eliminate_dBPOS(listo, WOB_db, RPM_db, DBTM_db,...
    DMEA_db, time_db, BPOS_db, ROP_db, DVER_db, dBPOS_db);


%Find maximum drillability
[list WOB_norm RPM_norm DBTM_norm DMEA_norm time_norm dBPOS_norm DVER_norm K Kmax]
= Calculate_Max_Drillability(list, WOB_cor, RPM_cor, DBTM_cor,...
    DMEA_cor, time_cor, dBPOS_cor, DVER_cor, a2, a5_ave, a6_ave);

%normalize with respect to maximum drillability
[normalized_K] = normalize(list, K, Kmax);

%Compute drillability in different formations
[Drillability Hardness norm_Drillability norm_Hardness] =
Calculate_Drillability_Hardness(list,...
```

```
    WOB_norm, RPM_norm, dBPOS_norm, DVER_norm, a2, a5_soft, a6_soft, a5_hard,
a6_hard, normalized_K);

%Compute average of hardness to achieve a smoother plot
[newlist H_AvePlot DMEA_AvePlot MaxH] = average_plot(list, norm_Hardness,
DMEA_norm);

%Normalize the average hardness
[H_NormPlot] = normalize(newlist, H_AvePlot, MaxH);

%The formation boundaries
depth_form = 1486;
[Balder] = formation(list, depth_form);
depth_form2 = 1555;
[Lista] = formation(list, depth_form2);
depth_form3 = 1655;
[Shetland] = formation(list, depth_form3);

%plot hardness vs measured depth
plot(H_NormPlot,DMEA_norm);
set(gca,'YDir','reverse');
xlabel('Hardness');
ylabel('Measured Depth [m]');
axis([-Inf Inf -Inf Inf]);
hold on
plot(norm_Hardness,Balder,'r');
hold on
plot(norm_Hardness,Lista,'r');
hold on
plot(norm_Hardness,Shetland,'r');
```

11.2 The executing functions

Twelve different executing functions have been applied.

11.2.1 Elimination of odd values of WOB

```
function [newlist WOB2 RPM2 DBTM2 DMEA2 time2 BPOS2 ROP2 DVER2] =
eliminate_WOB(list, WOB, RPM, DBTM, DMEA, time, BPOS, ROP, DVER)

j=1;
    for i = 1:1:list

            if WOB(i) > 5

                WOB2(j) = WOB(i);
                RPM2(j) = RPM(i);
                DBTM2(j) = DBTM(i);
                DMEA2(j) = DMEA(i);
                time2(j) = time(i);
                BPOS2(j) = BPOS(i);
                ROP2(j) = ROP(i);
                DVER2(j) = DVER(i);
                j=j+1;

            end

    end
    newlist = length(WOB2);
end
```

11.2.2 Elimination of odd values of RPM

```
function [newlist WOB2 RPM2 DBTM2 DMEA2 time2 BPOS2 ROP2 DVER2] =
eliminate_WOB(list, WOB, RPM, DBTM, DMEA, time, BPOS, ROP, DVER)

j=1;
```

```matlab
    for i = 1:1:list

            if WOB(i) > 5

                WOB2(j) = WOB(i);
                RPM2(j) = RPM(i);
                DBTM2(j) = DBTM(i);
                DMEA2(j) = DMEA(i);
                time2(j) = time(i);
                BPOS2(j) = BPOS(i);
                ROP2(j) = ROP(i);
                DVER2(j) = DVER(i);
                j=j+1;

            end

    end
    newlist = length(WOB2);
end
```

11.2.3 Elimination of odd values of DMEA

```matlab
function [newlist WOB2 RPM2 DBTM2 DMEA2 time2 BPOS2 ROP2 DVER2] =
eliminate_DMEA(list, WOB, RPM, DBTM, DMEA, time, BPOS, ROP, DVER)

j=1;
    for i = 1:1:list

            if DMEA(i) > 0

                WOB2(j) = WOB(i);
                RPM2(j) = RPM(i);
                DBTM2(j) = DBTM(i);
                DMEA2(j) = DMEA(i);
                time2(j) = time(i);
                BPOS2(j) = BPOS(i);
                ROP2(j) = ROP(i);
                DVER2(j) = DVER(i);
                j=j+1;

            end

    end

    newlist = length(WOB2);
end
```

11.2.4 Sort rows with respect to DMEA

```matlab
function [newlist WOB2 RPM2 DBTM2 DMEA2 time2 BPOS2 ROP2 DVER2] =
eliminate_DMEA(list, WOB, RPM, DBTM, DMEA, time, BPOS, ROP, DVER)

j=1;
    for i = 1:1:list

            if DMEA(i) > 0

                WOB2(j) = WOB(i);
                RPM2(j) = RPM(i);
                DBTM2(j) = DBTM(i);
                DMEA2(j) = DMEA(i);
                time2(j) = time(i);
                BPOS2(j) = BPOS(i);
                ROP2(j) = ROP(i);
                DVER2(j) = DVER(i);
                j=j+1;
```

```
            end

    end

    newlist = length(WOB2);
end
```

11.2.5 Compute average

```
function [newlist3 matrix3] = compute_average(list, matrix)

j=1;

    for i = 1:3:list-2

        matrix2(j,1) = (matrix(i,1) + matrix(i+1,1) + matrix(i+2,1))/3;
        matrix2(j,2) = (matrix(i,2) + matrix(i+1,2) + matrix(i+2,2))/3;
        matrix2(j,3) = (matrix(i,3) + matrix(i+1,3) + matrix(i+2,3))/3;
        matrix2(j,4) = (matrix(i,4) + matrix(i+1,4) + matrix(i+2,4))/3;
        matrix2(j,5) = (matrix(i,5) + matrix(i+1,5) + matrix(i+2,5))/3;
        matrix2(j,6) = (matrix(i,6) + matrix(i+1,6) + matrix(i+2,6))/3;
        matrix2(j,7) = (matrix(i,7) + matrix(i+1,7) + matrix(i+2,7))/3;
        matrix2(j,8) = (matrix(i,8) + matrix(i+1,8) + matrix(i+2,8))/3;

        j=j+1;

    end

    newlist2 = length(matrix2);

    j=1;
    for i = 1:3:newlist2-2

        matrix3(j,1) = (matrix2(i,1) + matrix2(i+1,1) + matrix2(i+2,1))/3;
        matrix3(j,2) = (matrix2(i,2) + matrix2(i+1,2) + matrix2(i+2,2))/3;
        matrix3(j,3) = (matrix2(i,3) + matrix2(i+1,3) + matrix2(i+2,3))/3;
        matrix3(j,4) = (matrix2(i,4) + matrix2(i+1,4) + matrix2(i+2,4))/3;
        matrix3(j,5) = (matrix2(i,5) + matrix2(i+1,5) + matrix2(i+2,5))/3;
        matrix3(j,6) = (matrix2(i,6) + matrix2(i+1,6) + matrix2(i+2,6))/3;
        matrix3(j,7) = (matrix2(i,7) + matrix2(i+1,7) + matrix2(i+2,7))/3;
        matrix3(j,8) = (matrix2(i,8) + matrix2(i+1,8) + matrix2(i+2,8))/3;
        j=j+1;
    end
```

11.2.6 Compute ΔBPOS

```
function [newlist WOB RPM DBTM DMEA time BPOS ROP DVER dBPOS] = Compute_dBPOS(list,
matrix)

j=1;
    for i = 2:1:list

        dBPOS(j) = ((matrix(i-1,6) - matrix(i,6))./15.*3600);
        WOB(j)  = matrix(i,1);
        RPM(j)  = matrix(i,2);
        DBTM(j) = matrix(i,3);
        DMEA(j) = (matrix(i,4) + matrix(i-1,4))/2;
        time(j) = matrix(i,5);
        BPOS(j) = (matrix(i,6) + matrix(i-1,6))/2;
        ROP(j)  = matrix(i,7);
        DVER(j) = matrix(i,8);
        j=j+1;

    end

    newlist = length(WOB);
```

```
end
```

11.2.7 Eliminate odd values of ΔBPOS

```
function [newlist WOB2 RPM2 DBTM2 DMEA2 time2 BPOS2 ROP2 DVER2 dBPOS2] =
eliminate_dBPOS(list, WOB, RPM, DBTM, DMEA, time, BPOS, ROP, DVER, dBPOS)

    j = 1;

    for i = 1:1:list

        if dBPOS(i) > 5 & dBPOS(i) < 100

        dBPOS2(j) = dBPOS(i);
        WOB2(j) = WOB(i);
        RPM2(j) = RPM(i);
        DBTM2(j) = DBTM(i);
        DMEA2(j) = DMEA(i);
        time2(j) = time(i);
        ROP2(j) = ROP(i);
        DVER2(j) = DVER(i);
        BPOS2(j) = BPOS(i);
        j=j+1;

        end

    end

    newlist = length(WOB2);

end
```

11.2.8 Calculate max drillability

```
function [newlist WOB2 RPM2 DBTM2 DMEA2 time2 dBPOS2 DVER2 K Kmax H] =
Calculate_Max_Drillability(list, WOB, RPM, DBTM, DMEA, time, dBPOS, a5, a6)

j=1;
    for i = 1:1:list

        if (DMEA(i)-DBTM(i)) < 0.1

            f5(j) = WOB(i)^a5; % Function of weight on bit
            f6(j) = RPM(i)^a6; % Function of rotary speed
            p(j) = f5(j).*f6(j).*f2(j);
            K(j) = dBPOS(i)./p(j); % Drillability
            H(j) = 1/K(j); % Hardness

            WOB2(j) = WOB(i);
            RPM2(j) = RPM(i);
            DBTM2(j) = DBTM(i);
            DMEA2(j) = DMEA(i);
            time2(j) = time(i);
            dBPOS2(j) = dBPOS(i);
            DVER2(j) = DVER(i);

            j=j+1;

        end

    end

    Kmax = max(K);
    newlist = length(K);
end
```

11.2.9 Normalize

```
function [A_norm] = normalize(list, A, Amax)

    for i = 1:1:list

        A_norm(i) = A(i)/Amax;

    end

end
```

11.2.10   Calculate drillability/hardness

```
function [K H normalized_K norm_H] = Calculate_Drillability_Hardness(list, WOB,
RPM, dBPOS, a5_hard, a6_hard, a5_soft, a6_soft,...
    norm_K)

    for i = 1:1:list

        if norm_K(i) < 0.5
            a5 = a5_hard;
            a6 = a6_hard;
        else
            a5 = a5_soft;
            a6 = a6_soft;
        end

            f5(i) = WOB(i)^a5; % Function of weight on bit
            f6(i) = RPM(i)^a6; % Function of rotary speed
            p(i) = f5(i).*f6(i);%.*f2(i);
            K(i) = dBPOS(i)./p(i); % Drillability
            H(i) = 1/K(i); % Hardness


    end

    MaxK = max(K);
    MaxH = max(H);

    for i = 1:1:list
        normalized_K(i) = K(i)/MaxK;
        norm_H(i) = H(i)/MaxH;
    end

end
```

11.2.11   Compute average hardness

```
function [newlist2 H_plot2 DMEA_plot2 MaxAveH2] = average_plot(list, H, DMEA)

j=1;

    for i = 1:3:list-2

        H_plot(j) = (H(i) + H(i+1) + H(i+2))/3;
        DMEA_plot(j) = (DMEA(i) + DMEA(i+1) + DMEA(i+2))/3;

        j=j+1;

    end

    MaxAveH = max(H_plot);
    newlist = length(H_plot);

    j=1;
    for i = 1:3:newlist-2

        H_plot2(j) = (H_plot(i) + H_plot(i+1) + H_plot(i+2))/3;
```

```matlab
        DMEA_plot2(j) = (DMEA_plot(i) + DMEA_plot(i+1) + DMEA_plot(i+2))/3;

        j=j+1;

    end

    MaxAveH2 = max(H_plot2);
    newlist2 = length(H_plot2);

end
```

11.2.12　　　　Drawing formation boundaries

```matlab
function [formation_list] = formation(list, depth)

    for i = 1:1:list
        formation_list(i) = depth;
    end

end
```